AD-A041 487 INDIANAPOLIS CENTER FOR ADVANCED RESEARCH IND FLUID--ETC F/G 20/4
THE MODELLING OF A TURBULENT NEAR WAKE USING THE INTERACTIVE HY--ETC(U)
1976 G D HUFFMAN, B S NG F44620-74-C-0065
UNCLASSIFIED FDL-77-001 AFOSR-TR-77-0181 NL

1 OF 1
ADA
041487

END

DATE
FILMED
7-77

INDIANAPOLIS CENTER FOR ADVANCED RESEARCH

INDIANA UNIVERSITY
PURDUE UNIVERSITY
at INDIANAPOLIS
SCHOOL OF SCIENCE

DEPARTMENT OF MATHEMATICAL SCIENCES

AIR FORCE OFFICE OF SCIENTIFIC RESEARCH (AFSC)
NOTICE OF TRANSMITTAL TO DDC
This technical report has been reviewed and is approved for public release IAW AFR 190-12 (7b).
Distribution is unlimited.
A. D. BLOSE
Technical Information Officer

SECURITY CLASSIFICATION OF THIS PAGE (When Data Entered)

REPORT DOCUMENTATION PAGE

READ INSTRUCTIONS BEFORE COMPLETING FORM

1. REPORT NUMBER: AFOSR-TR-77-0181	2. GOVT ACCESSION NO.
3. RECIPIENT'S CATALOG NUMBER	
4. TITLE (and Subtitle): THE MODELLING OF A TURBULENT NEAR WAKE USING THE INTERACTIVE HYPOTHESIS	5. TYPE OF REPORT & PERIOD COVERED: FINAL, 1 April 1974-1 July 1976
6. PERFORMING ORG. REPORT NUMBER	
7. AUTHOR(s): G D UFFMAN, B S NG	8. CONTRACT OR GRANT NUMBER(s): F44620-74-C-0065
9. PERFORMING ORGANIZATION NAME AND ADDRESS: INDIANAPOLIS CENTER FOR ADVANCED RESEARCH, FLUID DYNAMICS LABORATORIES, 909 WEST NEW YORK ST; INDIANAPOLIS, IN 46202	10. PROGRAM ELEMENT, PROJECT, TASK AREA & WORK UNIT NUMBERS: 681307, 9781-01, 61102F
11. CONTROLLING OFFICE NAME AND ADDRESS: AIR FORCE OFFICE OF SCIENTIFIC RESEARCH/NA, BLDG 410, BOLLING AIR FORCE BASE, D C 20332	12. REPORT DATE: 1976
	13. NUMBER OF PAGES: 44
14. MONITORING AGENCY NAME & ADDRESS (if different from Controlling Office): TDL-77-001	15. SECURITY CLASS. (of this report): UNCLASSIFIED
	15a. DECLASSIFICATION/DOWNGRADING SCHEDULE

16. DISTRIBUTION STATEMENT (of this Report)

Approved for public release; distribution unlimited.

17. DISTRIBUTION STATEMENT (of the abstract entered in Block 20, if different from Report)

18. SUPPLEMENTARY NOTES

19. KEY WORDS (Continue on reverse side if necessary and identify by block number)

NEAR WAKE
ASYMMETRIC WAKE
TURBULENT WAKE MODELLING

20. ABSTRACT (Continue on reverse side if necessary and identify by block number)

A semi-empirical mathematical model for a turbulent near wake has been developed within the framework of an "interaction hypothesis" suggested by Bradshaw. The near wake behind an airfoil has been treated as a "complex" shear flow consisting of two neighboring simple shear layers with distinct but overlapping shear stress profiles of opposite signs. The present model utilizes the mean momentum and continuity equations together with two shear stress transport equations derived from the turbulent kinetic energy equation. By relating the shear stresses to the local turbulence equantities, closure for the governing systems is achieved

DD FORM 1 JAN 73 1473 EDITION OF 1 NOV 65 IS OBSOLETE

UNCLASSIFIED
SECURITY CLASSIFICATION OF THIS PAGE (When Data Entered)

410 273

without the use of the eddy viscosity concept. The shear stress is therefore no longer required to vanish at the velocity extremum. The model has been compared to the experimental data of Chevray and Kovasznay and good agreement has been obtained. A comparison with the asymmetric cascade wake data of Raj and Lakshminarayana is also presented. Our calculations have validated the basic philosophy of an interactive approach in the study of near wakes. However, it also clearly demonstrates that the accouracy of certain empirical functions used to define the turbulence structure has a direct impact on the success of this or any other calculation method.

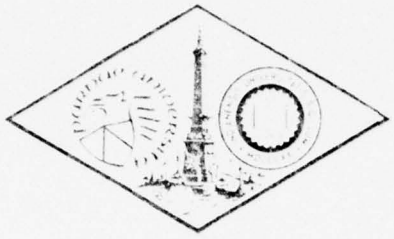

Indianapolis Center for Advanced Research

THE MODELLING OF A TURBULENT NEAR WAKE USING THE INTERACTIVE HYPOTHESIS

AF Contract Number
F44620-74-C-0065

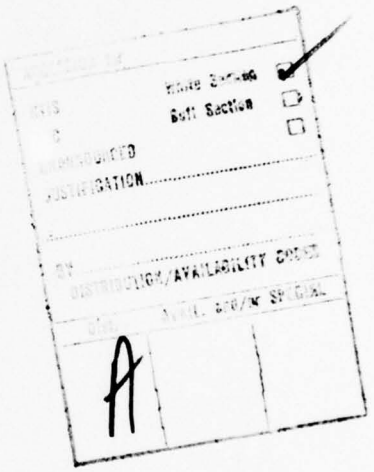

Report Number FDL-77-001

G. D. Huffman

B. S. Ng

Final Report 1976

This research was sponsored by the Air Force Office of Scientific Research (AFSC) United States Air Force, under Contract F44620-74-C-0065. The United States Government is authorized to reproduce and distribute reprints for governmental purposes notwithstanding any copyright notation hereon.

INDIANA UNIVERSITY PURDUE UNIVERSITY at INDIANAPOLIS

SCHOOL OF SCIENCE

Department of Mathematical Sciences

TABLE OF CONTENTS

LIST OF FIGURES

ABSTRACT

A semi-empirical mathematical model for a turbulent near wake has been developed within the framework of an "interaction hypothesis" suggested by Bradshaw. The near wake behind an airfoil has been treated as a "complex" shear flow consisting of two neighboring simple shear layers with distinct but overlapping shear stress profiles of opposite signs. The present model utilizes the mean momentum and continuity equations together with two shear stress transport equations derived from the turbulent kinetic energy equation. By relating the shear stresses to the local turbulence quantities, closure for the governing systems is achieved without the use of the eddy viscosity concept. The shear stress is therefore no longer required to vanish at the velocity extremum. The model has been compared to the experimental data of Chevray and Kovasznay and good agreement has been obtained. A comparison with the asymmetric cascade wake data of Raj and Lakshminarayana is also presented. Our calculations have validated the basic philosophy of an interactive approach in the study of near wakes. However, it also clearly demonstrates that the accuracy of certain empirical functions used to define the turbulence structure has a direct impact on the success of this or any other calculation method.

INTRODUCTION

One of the primary objectives of the present research program is to develop an accurate and effective technique for predicting aerodynamically induced vibrations of rotor and stator blades in turbomachines. From a theoretical standpoint, an essential step towards the development of such a method requires a realistic modelling of the flow through an annular cascade of airfoils. The resulting problem is, of course, three-dimensional, but it can be substantially simplified if we assume axial symmetry in the time-averaged basic flow so that a two-dimensional analysis in the circumferential or blade-to-blade stream surface is possible. Within this general context, the turbulent near wake behind any one airfoil constitutes but a small part of the overall cascade flow field. Nevertheless, the structure of a near wake plays a decisive role in determining the aerodynamic forcing function which will be needed for any subsequent cascade gust calculations.

Despite recent advances in numerical methods dealing with turbulent boundary layers,[1] little progress has been made in the modelling of an asymmetric turbulent near wake. This is in part due to the fact that the state of the art in turbulent modelling is such that a large amount of empiricism is often required to insure the success of any prediction method. In the case of a near wake formed by the coalescence of two turbulent boundary layers with opposite shear stresses, very little is known about the mechanism of their interaction. Moreover, for an asymmetric wake, the point of zero Reynolds stress does not necessarily coincide with the point of zero velocity gradient. Any attempt to obtain closure for the governing equations by using a simple eddy viscosity model for the shear stress will therefore encounter difficulties. It is the purpose of this work then to outline a method by which these problems can be resolved.

In important element in our present analysis is the "interaction hypothesis" first proposed by Bradshaw, et. al. in conjunction with the study of duct flow.[2]

Within the context of this hypothesis, a near wake can be regarded as an interaction between two neighboring simple shear layers with distinct but possibly overlapping shear stress profiles of opposite signs (cf. Figure 1). If the interaction is such that the *turbulence structure* in each layer is essentially unaffected by the presence of the adjacent layer, a superposition of the two shear stress fields for the purpose of calculating the net Reynolds stress is then possible. Moreover, by relating the shear stresses to the local turbulent quantities, as it has been suggested by Bradshaw, Ferriss and Atwell,[3] two shear stress transport equations can be derived from the turbulent kinetic energy equation. Closure for the governing system is therefore achieved without making use of the eddy viscosity concept.

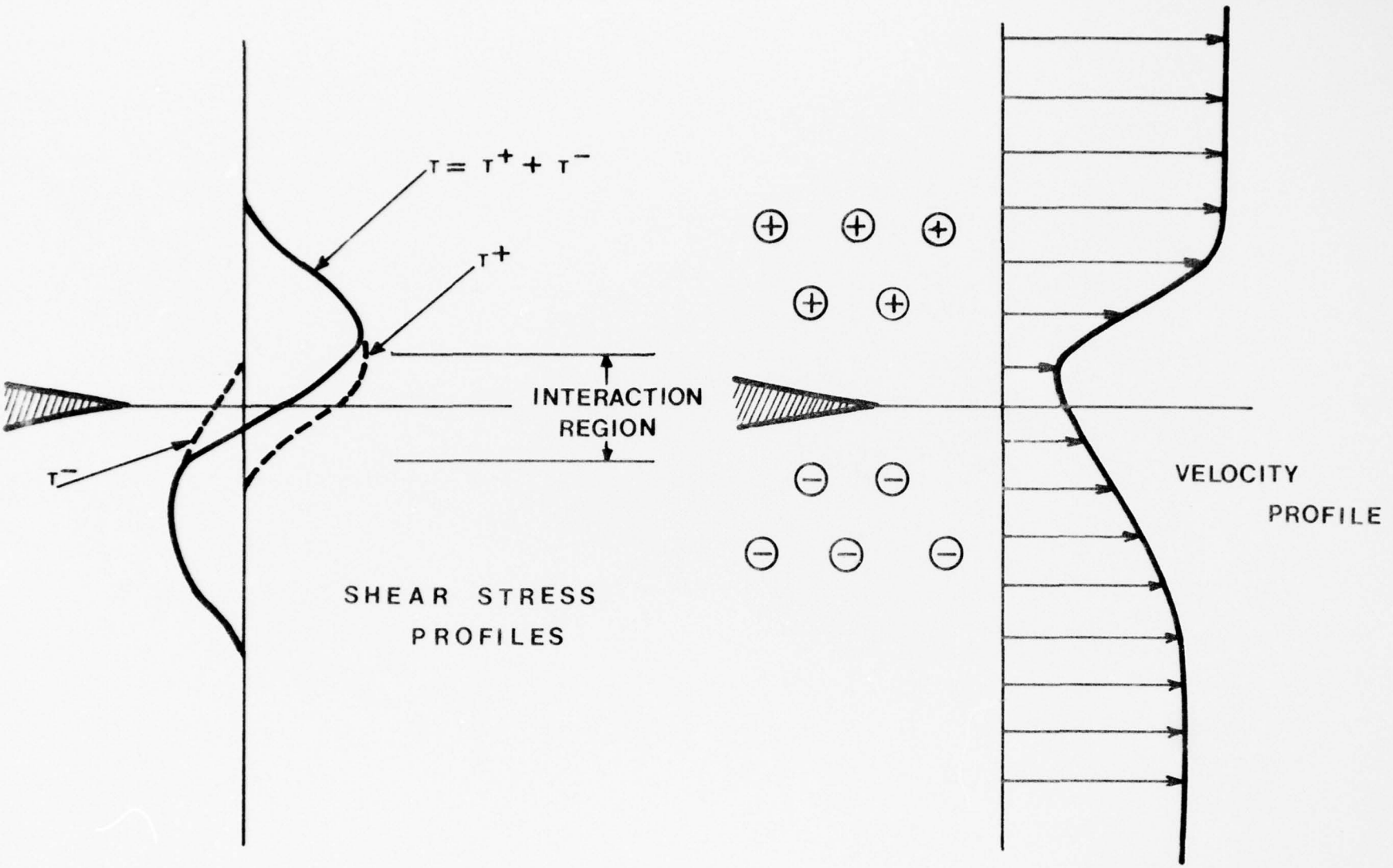

FIGURE 1. THE "INTERACTION HYPOTHESIS".

BASIC FORMULATION: INTERACTIVE APPROACH

In order to explore the validity of the interaction approach, our investigation has been confined to a prototype model which includes only the essential physical details. The fluid is initially assumed to be incompressible. Furthermore, due to the magnitude of the Reynolds number usually encountered in turbomachine/internal flow applications, the flow is also expected to satisfy the boundary layer approximation and the viscous stresses have been ignored when compared to the Reynolds stresses. The momentum and continuity equations are then given by

$$\left(U \frac{\partial}{\partial x} + V \frac{\partial}{\partial y} \right) U = U_\infty \frac{dU_\infty}{dx} + \frac{\partial \tau}{\partial y} , \qquad (1)$$

and

$$\frac{\partial U}{\partial x} + \frac{\partial V}{\partial y} = 0. \qquad (2)$$

The Cartesian coordinate system for these equations is chosen such that the x-axis is tangent to the mean camber line of an upstream airfoil at the trailing edge; x is equal to 0 at the trailing edge and positive in the downstream direction. The time-averaged velocity components along the x and y axes are then given by U and V, respectively. The free stream velocity U_∞ in the pressure gradient term of equation (1) is to be replaced by $U_{+\infty}$ or $U_{-\infty}$, depending on whether $y > y_c$ or $y < y_c$, where $y_c(x)$ is the locus of the velocity minimum. Physically, our prototype problem can be envisioned as that of a two-dimensional asymmetric wake behind an airfoil or a flat plate, formed by the coalescence of the upper and lower surface boundary layers having possibly different characteristics. In our present notation, the usual shear stress is replaced by τ = (shear stress)/(density) $= -\overline{uv}$, where u and v are velocity fluctuations and the overbar denotes a time average.

According to the interaction hypothesis, we can further write

$$\tau = \tau^{+} + \tau^{-}$$

such that τ^{+} is the dominant shear stress in the region of positive shear--nominally where $y > y_c$--and vice versa for τ^{-}. In order to obtain a tractable system, certain assumptions must be made to secure closure for equations (1) and (2). Using the Bradshaw-Ferriss-Atwell turbulence model[3] we define two sets of empirical functions, (a_1^{+}, G^{+}, L^{+}) and (a_1^{-}, G^{-}, L^{-}), such that

$$a_1^{\pm} = \frac{\tau^{\pm}}{\overline{q^2}} \quad , \tag{3}$$

$$G = \frac{(\overline{p'v} + \frac{1}{2}\overline{q^2 v})}{|\tau^{\pm}||\tau_m^{\pm}|^{1/2}} \quad , \tag{4}$$

and

$$L^{\pm} = \frac{\tau^{\pm}|\tau^{\pm}|^{1/2}}{\varepsilon} \quad . \tag{5}$$

The relations (3) - (5) are equivalent to assuming that (i) the local shear stress is proportional to the turbulent intensity $\overline{q^2}$; (ii) the energy diffusion is directly proportional to the local shear stress with a factor depending on the maximum of the shear stress, τ_m, and (iii) the dissipation rate ε is determined by local shear stress and a length scale L. With equations (3), (4) and (5), the structure of turbulence is defined in terms of relations between turbulence quantities and it is thus independent of the mean flow. It has been observed that the above assumptions are quite valid over a wide range of pressure gradients, Mach number, Reynolds number and appear to be rather insensitive to rapid changes in the mean flow.[4,5] This will, of course, enable the present method to be extended to a wide variety of mean flow conditions, often without the need for extra data. On substituting (3), (4) and (5) into the exact turbulent energy equation, we can derive two transport equations for τ^{+} and τ^{-} of the

form

$$\left(U\frac{\partial}{\partial x} + V\frac{\partial}{\partial y}\right)\left(\frac{\tau^{\pm}}{2a_1^{\pm}}\right) = \tau^{\pm}\frac{\partial U}{\partial y} \mp \frac{\partial}{\partial y}\left(G^{\pm}\tau^{\pm}|\tau_m^{\pm}|^{1/2}\right) \mp \frac{\tau^{\pm}|\tau^{\pm}|^{1/2}}{L^{\pm}} \quad . (6)$$

The system consisting of equations (1), (2) and (6) is now closed provided that the empirical functions can be determined experimentally. A schematic representation of these functions is given in Figure 2. Conceptually, the two sets of empirical functions are to be regarded as distinct, but in fact they are qualitatively the same except for changes in signs and their dependence on y as illustrated in Figures 2 and 3. It must be emphasized that the success of the present approach, regardless of the method used in solving the governing system of equations is then dependent on the accuracy of $(a_1^{\pm}, G^{\pm}, L^{\pm})$. The details of the empirical functions used in our calculations are discussed in the RESULTS AND DISCUSSION section. In addition to equations (1), (2) and (6), certain initial and boundary conditions must be specified.

On noting that the genesis of a near wake is effected by the merging of two surface boundary layers at the trailing edge where $x = 0$, the natural initial conditions for an airfoil with zero trailing edge thickness are therefore given by

$$U = U(0,y) \quad , \tag{7}$$

$$V = V(0,y) \quad , \tag{8}$$

$$\tau^{+} = \begin{cases} \tau^{+}(0,y) & , \quad y \geq 0 \\ 0 & , \quad y < 0 \end{cases} \tag{9}$$

and

$$\tau^{-} = \begin{cases} 0 & , \quad y > 0 \\ \tau^{-}(0,y) & , \quad y \leq 0 \end{cases} \tag{10}$$

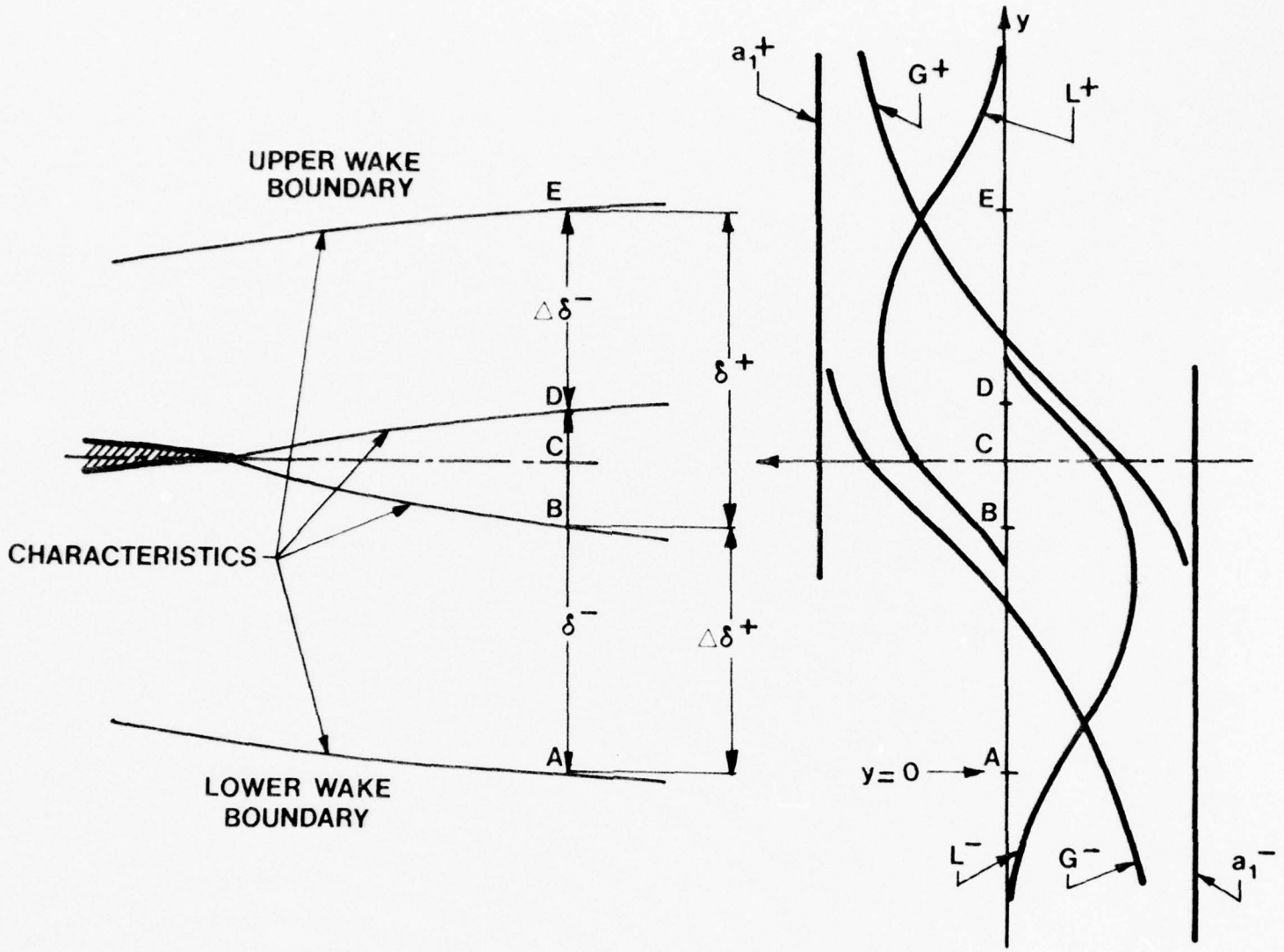

FIGURE 2. A SCHEMATIC REPRESENTATION OF THE EMPIRICAL FUNCTIONS

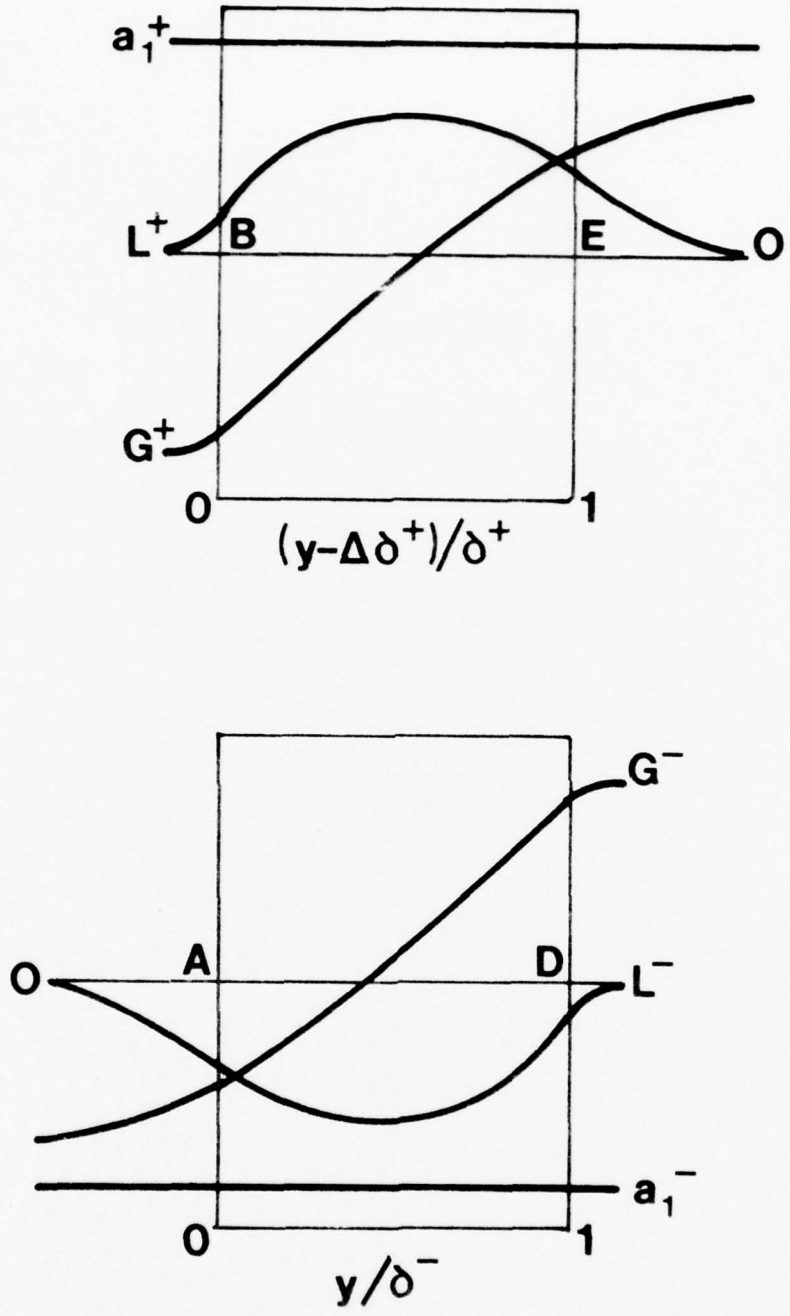

FIGURE 3. THE RELATION BETWEEN (a_1^+, G^+, L^+) and (a_1^-, G^-, L^-).

where the velocity profiles $U(0,y)$ and $V(0,y)$, and the shear stress profiles $\tau^+(0,y)$ and $\tau^-(0,y)$ are ideally supplied by an upstream boundary layer calculation or measured directly from experiments. For $x > 0$, we shall also require that $V(x,y_c) = 0$, when $y_c = 0$ for the symmetric case.

The boundary conditions for the present problem are

$$\left.\begin{array}{l} U \to U_{+\infty} \\ \tau^+ \to 0 \end{array}\right\} \quad \text{as } y \to +\infty \ , \tag{11}$$

and

$$\left.\begin{array}{l} U \to U_{-\infty} \\ \tau^- \to 0 \end{array}\right\} \quad \text{as } y \to -\infty \ . \tag{12}$$

A careful examination of the turbulent shear stress equations also indicates that τ^+ should vanish almost immediately after crossing into the region dominated by negative shear. In fact, on noting that the governing system is hyperbolic, it is possible to determine two characteristics, Γ^+ and Γ^-, emanating from the trailing edge such that $\tau^+ \equiv 0$ in a region bounded by Γ^- and the lower edge of the wake, and vice versa for τ^-. In differential form, these characteristics are given by

$$\Gamma^{\pm}: \ \frac{dy}{dx} = \tan \gamma_{\pm}, \text{ and } y(0) = 0 \ , \tag{13}$$

where

$$\tan \gamma_{\pm} = \frac{V \pm a_1^{\pm} G^{\pm} |\tau_m^{\pm}|^{1/2} \pm [(a_1^{\pm} G^{\pm})^2 |\tau_m^{\pm}| + 2a_1^{\pm} \tau^{\pm}]^{1/2}}{U} \ .$$

Hyperbolicity has indeed been fully exploited in the work of Bradshaw, et. al.(see, e.g., references 2, 3 and 4). In the present analysis, however, the characteristics associated with the governing system play a relatively minor role. They are useful in so far as providing a conceptual framework within which the precise boundaries of the interacting shear layers can be defined for

the purpose of scaling the empirical functions (cf. Figures 2 and 3). On the other hand, the conditions that τ^+ and τ^- be respectively zero in most of the regions of negative and positive shear will be automatically satisfied if we require that

$$\tau^+ \to 0 \quad \text{as} \quad y \to -\infty \ , \tag{14}$$

and

$$\tau^- \to 0 \quad \text{as} \quad y \to +\infty \ . \tag{15}$$

The explicit use of characteristics in specifying boundary conditions is therefore unnecessary. It is useful to note here a few key points of the interactive analysis:

(i) Due to the inclusion of the boundary layer profiles at the trailing edge as initial conditions, the observed flow asymmetry is being dealt with directly.

(ii) Since the near wake is highly dependent upon the structure of the lower and upper surface boundary layers, the interaction approach is expected to produce better results than any similarity methods in which the loss of initial conditions is implicit in the zero initial wake-width assumption.

(iii) The (indirect) use of the turbulent energy equation leads to the incorporation of advective and diffusive effects in the energy budget, in addition to the usual balance between production and dissipation of turbulence. The "past history" of the turbulence is therefore explicitly taken into account. In a highly turbulent and rapidly varying flow region, such as a near wake, this consideration will have a direct bearing on the accuracy of the present model.

(iv) The decomposition of the net shear stress profile into τ^+ and τ^-, each of which satisfies a separate transport equation, enables us to circumvent the usual difficulties associated with any complex shear flow having an extremum in its velocity profile.

(v) It is also of interest to point out that past experience with boundary layers and duct flow indicates that the empirical functions exhibit a remarkable measure of universality.[5] It is expected that the corresponding functions for near wakes, once determined, will be canonical, to some extent, to the present class of flow. In any internal flow applications, a particular cascade geometry and the angle of attack or incidence of the airfoil will only influence the near wake solution through the initial and boundary conditions.

In the foregoing analysis, the fluid has been assumed to be incompressible. This simplification can be removed without added complexities if we invoke Morkovin's hypothesis that the turbulence structure -- defined in our case by the empirical functions -- is unaffected by compressibility when the Mach number fluctuation is much less than unity. This approach has been found to be quite satisfactory by Bradshaw[6] for boundary layers on adiabatic walls at free-stream Mach numbers up to 4. Thus, using an order of magnitude analysis identical to that of Bradshaw, the mean momentum, continuity, and turbulent kinetic energy equations for adiabatic compressible flow take on the following simplified forms:

$$U \frac{\partial U}{\partial x} + \left(V + \frac{\overline{\rho' v}}{\rho}\right) \frac{\partial U}{\partial y} = -\frac{1}{\bar{\rho}} \frac{\partial \bar{p}}{\partial x} + \frac{1}{\bar{\rho}} \frac{\partial \bar{\rho}\tau}{\partial y} \qquad (16)$$

$$\frac{\partial \bar{\rho} U}{\partial x} + \frac{\partial}{\partial y} (\bar{\rho} V + \overline{\rho' v}) = 0 \tag{17}$$

$$\bar{\rho} U \frac{\partial \frac{1}{2}\overline{q^2}}{\partial x} + \bar{\rho} \left(V + \frac{\overline{\rho' v}}{\bar{\rho}}\right) \frac{\partial \frac{1}{2}\overline{q^2}}{\partial y} = \tau \frac{\partial U}{\partial y} - \frac{\partial}{\partial y} \left(\overline{p' v} + \frac{1}{2} \bar{\rho} \cdot \overline{q^2 v} + \frac{1}{2} \overline{\rho' q^2 v}\right)$$

$$- D - \bar{\rho} \varepsilon \tag{18}$$

where

$$D \equiv \frac{tr}{a_1} (\gamma - 1) \frac{M_\infty^2}{U} \cdot \bar{\rho} \tau \frac{\partial \tau}{\partial y} \quad , \tag{19}$$

$r = 0.886$ being the recovery factor, t a constant such that $tr/a_1 \sim 7$, $\gamma = 1.4$ the ratio of specific heats and M_∞ the free stream Mach number. All the symbols in equations (16) - (19) denote the same quantities as in the incompressible case, with ρ' being the density fluctuating. On replacing $(V + \overline{\rho' v}/\bar{\rho})$ by V, using the Crocco relation $c_p T + rU^2/2$ to find the mean temperature and hence the mean density, and making the assumptions that

$$\tau = \tau^+ + \tau^- \tag{20}$$

$$a_1^{\pm} = \tau^{\pm}/\overline{q^2} \tag{21}$$

$$G^{\pm} = \frac{\left(\overline{p' v} + \frac{1}{2} \overline{\rho q^2 v} + \frac{1}{2} \overline{\rho' q^2 V}\right)}{|\tau^{\pm}| \, |\tau_m^{\pm}|^{1/2}} \tag{22}$$

$$L^{\pm} = \tau^{\pm} |\tau^{\pm}|^{1/2} / \varepsilon \tag{23}$$

as in the incompressible case, the four equations for the dependent variables U, V, τ^+ and τ^- are

$$U \frac{\partial U}{\partial x} + \left[V - r(\gamma - 1) M_\infty^2 \frac{\tau}{U}\right] \frac{\partial U}{\partial y} = - \frac{U^2}{\gamma M_\infty^2} \cdot \frac{1}{\bar{p}} \frac{d\bar{p}}{dx} + \frac{\partial \tau}{\partial y} \tag{24}$$

$$\frac{\partial U}{\partial x}\left[1 + r(\gamma - 1)M_\infty^2\right] + \frac{\partial U}{\partial y} \cdot \frac{V}{U} \cdot r(\gamma - 1)M_\infty^2 + \frac{\partial V}{\partial y} + \frac{U}{\bar{p}} \frac{d\bar{p}}{dx} = 0 \qquad (25)$$

$$\frac{U}{2a_1^{\pm}} \frac{\partial \tau^{\pm}}{\partial x} + \left[\frac{V}{2a_1^{\pm}} + \frac{tr}{a_1^{\pm}} (\gamma - 1)M_\infty^2 \frac{\tau^{\pm}}{U}\right] \frac{\partial \tau^{\pm}}{\partial y} =$$

$$\tau^{\pm}\left[1 \pm G^{\pm}|\tau_m^{\pm}|^{1/2} r(\gamma - 1) \frac{M_\infty^2}{U}\right] \frac{\partial U}{\partial y}$$

$$\mp \frac{\partial}{\partial y} (G^{\pm}\tau^{\pm}|\tau_m|^{\pm}) - \frac{\tau^{3/2}}{L} \quad , \qquad (26) - (27)$$

where the coefficient in the pressure gradient term of equation (24) has been rewritten such that the mean density does not appear explicitly. The free stream Mach number M_∞ in equations (24) and (25) must be replaced by $M_{+\infty}$ or $M_{-\infty}$, depending on the shear region, and the pressure gradient must also be adjusted accordingly. It can easily be shown that equations (24) - (27) are again hyperbolic and they are reducible to the incompressible equations when $M \to 0$. The solution algorithm to be discussed in the next section is therefore equally applicable to the compressible case with only minor modifications.

SOLUTION ALGORITHM

A number of very effective algorithms have been developed in recent years for solving quasi-linear hyperbolic systems of the form given by equations (1), (2) and (6). In the work of Bradshaw, et.al. on turbulent boundary layers,[3] the method of characteristics was adopted to solve a somewhat simpler system of three equations involving the dependent variables U, V and τ. The advantages of such an approach are that the resulting numerical scheme is essentially explicit, and that the well-known Courant-Friedrichs-Lewy criterion provides a clear cut limit to the x-step that can be taken to insure numerical stability. The uncoupling of the continuity equation from the remaining system in that case also effectively reduces the problem to one of only two unknowns--namely, U and τ--so that the characteristic angles at each point in the flow can be conveniently determined by a second-order algebraic equation.

For our present purpose, a direct generalization of the method of characteristics to deal with equations (1), (2) and (6) is, of course, possible but has been found to be somewhat cumbersome. Despite the fact that V can again be uncoupled, the determination of the characteristic angles now requires the solution of essentially a third-order algebraic equation. An attempt to circumvent this difficulty has since been discussed by Bradshaw, Dean and McEligot in conjunction with their work on duct flow.[2] Due to the rather weak coupling of the governing system, it has been suggested that the two turbulent shear stress equations can be solved separately using the velocity profile at the previous x-step as a first approximation. The resulting τ^+ and τ^- are then summed and a new velocity profile is then calculated. Accuracy can presumably be improved through iteration. For our purpose, however, we find it convenient to formulate a more direct numerical scheme based on the general finite difference approach similar to the one devised by Ferriss.[7]

In anticipation of the rapidly varying velocity profiles in the inner wake region similar to those encountered in boundary layers, a mesh of variable grid size in the normal directions has been adopted for the present analysis. The y-steps are gradated outward from the x-axis in the form of a geometric sequence such that

$$(\Delta y)_j = \alpha(\Delta y)_{j-1} = \alpha^{|j|}(\Delta y)_0 ,$$

where

$$(\Delta y)_j = y_{j+1} - y_j , \tag{28}$$

and

$$y_1 = -y_0 = \frac{(\Delta y)_0}{2} .$$

The geometric ratio α is usually taken to be of the order of 1.05. We shall also denote the boundary grid points for the lower and upper wake edges respectively by y_{-L} and y_M. The total number of interior grid points at any given x-station is then given by

$$J = L + M - 1 .$$

The required numerical scheme for solving equations (1), (2) and (6) can now be formulated in terms of difference quotients within a typical computation cell consisting of two adjacent mesh rectangles as shown in Figure 4. For any function f(x,y) which is at least twice differentiable in y, the second-order-correct finite difference approximation to the partial derivative of f with respect to y at (x_i, y_i) is then given by

$$\left(\frac{\partial f}{\partial y}\right)_{i,j} = \frac{f_{i,j+1} - (1-\lambda^2) f_{i,j} - \lambda^2 f_{i,j-1}}{\alpha^{|j|}(1+\lambda)(\Delta y)_0} , \tag{29}$$

where

$$\lambda = \begin{cases} \alpha & \text{for} \quad j \geq 1 \\ \alpha^{-1} & \text{for} \quad j < 1 \end{cases} .$$

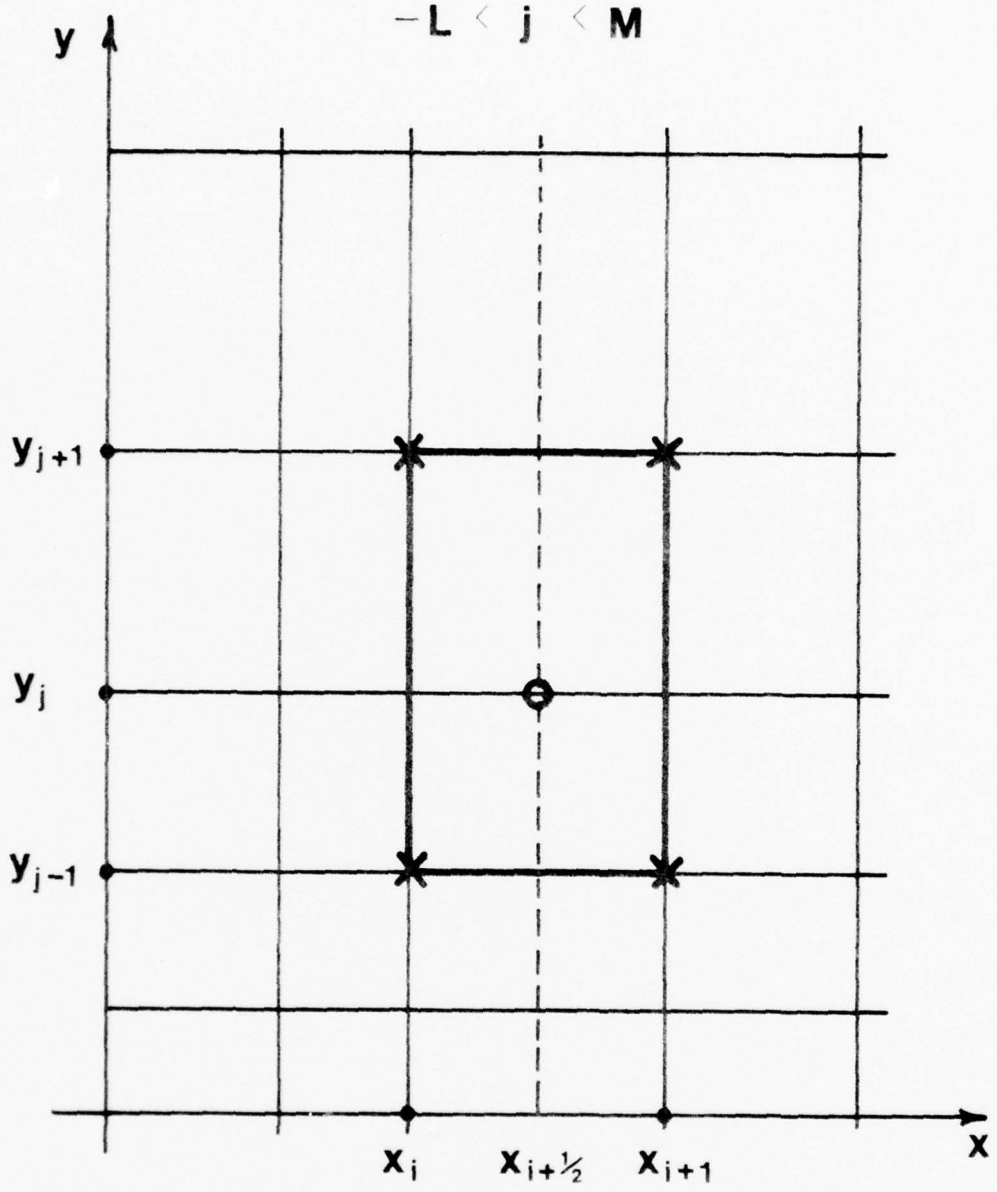

FIGURE 4. A TYPICAL COMPUTATION CELL FOR DIFFERENCE APPROXIMATIONS (29) AND (30)

In the case of a logarithmic function of y, it can be shown that the error associated with an approximation of the form given by (29) remains constant throughout the entire grid despite the increase in y-step size in the outer regions (e.g., reference 8). A"centered"difference equation is used to approximate the partial derivative of f with respect to x. Thus we have

$$\left(\frac{\partial f}{\partial x}\right)_{i+1/2,j} \approx \frac{f_{i+1,j} - f_{i,j}}{(\Delta x)_i} \quad , \tag{30}$$

where

$$x_{i+1/2} = \frac{x_{i+1} + x_i}{2} \quad ,$$

and

$$(\Delta x)_i = x_{i+1} - x_i \quad .$$

Moreover, it is useful to note that

$$\left(\frac{\partial f}{\partial y}\right)_{i+1/2,j} \approx \left\{\left(\frac{\partial f}{\partial y}\right)_{i+1,j} + \left(\frac{\partial f}{\partial y}\right)_{i,j}\right\} \Big/ 2. \tag{31}$$

The finite difference analog to the governing system can now be derived by replacing the partial derivatives in equations (1), (2) and (6) with their corresponding approximations given by (30) and (31). For this purpose, we now define

$$E^{(r)}_{i,j} = \begin{bmatrix} e^{+}_{i,j,r} & -\tau^{+}_{i,j} & 0 \\ 1 & -V_{i,j} & 1 \\ 0 & -\tau^{-}_{i,j} & e^{-}_{i,j,r} \end{bmatrix} , \tag{32}$$

$$H_{i,j} = \begin{bmatrix} h_{i,j}/a^{+}_{1} & 0 & 0 \\ 0 & 2h_{i,j} & 0 \\ 0 & 0 & h_{i,j}/a^{-}_{1} \end{bmatrix} , \tag{33}$$

where

$$e^{\pm}_{i,j,r} = \frac{V^{\pm}_{i,j}}{2a_1^{\pm}} \pm G^{\pm}_{i+1,j+r} \left|\tau^{\pm}_m\right|^{1/2}_i \qquad r = -1,\ 0,\ 1, \tag{34}$$

and

$$h_{i,j} = \frac{(\Delta y)_0}{(\Delta x)_i} \alpha^{|j|} (\lambda+1)\ U_{i,j} \ . \tag{35}$$

It can then be shown that around the point $(x_{i+1/2}, y_j)$, equations (1), (2) and (6) are reducible to

$$A_{i,j}\overleftarrow{s}_{i+1,j-1} + B_{i,j}\overleftarrow{s}_{i+1,j} + C_{i,j}\overleftarrow{s}_{i+1,j+1} = \overleftarrow{d}_{i,j} \tag{36}$$

where

$$A_{i,j} = -\lambda^2 E_{i,j}^{(-1)} \ , \tag{37}$$

$$B_{i,j} = -(1-\lambda^2) E_{i,j}^{(0)} - H_{i,j} \ , \tag{38}$$

$$C_{i,j} = E_{i,j}^{(1)} \tag{39}$$

and

$$\overleftarrow{s}_{i,j} = \begin{bmatrix} \tau^{+}_{i,j} \\ U_{i,j} \\ \tau^{-}_{i,j} \end{bmatrix} \tag{40}$$

The inhomogeneous term $d_{i,j}$ is given by

$$\overleftarrow{d}_{i,j} = -A_{i,j}\overleftarrow{s}_{i,j-1} + [(1-\lambda^2)E_{i,j}^{(0)} - H_{i,j}]\overleftarrow{s}_{i,j} - C_{i,j}\overleftarrow{s}_{i,j+1} + \overleftarrow{q}_{i,j} \tag{41}$$

where

$$\overleftarrow{q}_{i,j} = (\Delta y)_0 \alpha^{|j|} (\lambda+1) \begin{bmatrix} \tau^{+}_{i,j}\left|\tau^{+}_{i,j}\right|^{1/2}/L^{+}_{i,j} \\ U_{i+1/2,\infty}(U_{i+1,\infty} - U_{i,\infty})/\Delta x \\ \tau^{-}_{i,j}\left|\tau^{-}_{i,j}\right|^{1/2}/L^{-}_{i,j} \end{bmatrix} \ . \tag{42}$$

In equation (42), the edge velocity $U_{,\infty}$ must be replaced by $U_{,+\infty}$ or $U_{,-\infty}$, depending on whether $y_j > y_c$ or $y_j < y_c$. In the course of deriving equation (36), we have also linearized the corresponding equations by approximating the coefficients involving U, V, τ^+ or τ^- by their values at x_i, which are taken to be known. The non-linear version may be recovered, if needed, by replacing $i + 1/2$ for the i-indices of those dependent variables appearing in equations (32) - (35). At any given x-station, the J interior grid points then generate 3J equations with the same number of unknowns. The resulting system can be written in the following compact form:

$$\underbrace{\begin{bmatrix} B_{-L+1} & C_{-L+1} & & & & & & & \\ A_{-L+2} & B_{-L+2} & C_{-L+2} & & & & & & \\ & A_{-L+3} & B_{-L+3} & C_{-L+3} & & & 0 & & \\ & & \ddots & \ddots & \ddots & & & & \\ & & & A_{-1} & B_{-1} & C_{-1} & & & \\ & & & & A_0 & B_0 & C_0 & & \\ & & & & & A_1 & B_1 & C_1 & \\ & & & & & & \ddots & \ddots & \ddots \\ & & 0 & & & & & A_{M-3} & B_{M-3} & C_{M-3} \\ & & & & & & & & A_{M-2} & B_{M-2} & C_{M-2} \\ & & & & & & & & & A_{M-1} & B_{M-1} \end{bmatrix}}_{\mathcal{M}} \underbrace{\begin{bmatrix} s_{-L+1} \\ s_{-L+2} \\ s_{-L+3} \\ \vdots \\ s_{-1} \\ s_0 \\ s_1 \\ \vdots \\ s_{M-3} \\ s_{M-2} \\ s_{M-1} \end{bmatrix}}_{s} = \underbrace{\begin{bmatrix} d_{-L+1} - A_{-L+1} s_{-L} \\ d_{-L+2} \\ d_{-L+3} \\ \vdots \\ d_{-1} \\ d_0 \\ d_1 \\ \vdots \\ d_{M-3} \\ d_{M-2} \\ d_{M-1} - C_{M-1} s_M \end{bmatrix}}_{d} \tag{43}$$

where the i-indices have been omitted for clarity. The boundary conditions at y_{-L} and y_M are incorporated through the inhomogeneous vector $\underset{\sim}{d}$. Before the above linear system is actually solved, however, a modification is desirable. On noting that the downstream shear stress distributions of both the top and bottom shear layers should vanish in most of the regions of opposite shear due to zero upstream conditions, it is possible to calculate τ^+ and τ^- only at those grid points where they are non-zero. The advantage of this approach is that it results in a reduction of the number of equations and therefore the size of the matrix M. A more important consequence is that we are dispensed with the need to define and justify the empirical functions too far beyond the boundaries within which the top and lower shear layers are confined. On the other hand, care must be exercised to allow for the growth of the shear layers. For this purpose, whenever a shear stress profile is computed, the magnitude of the shear stress at an edge grid point is checked to determine whether certain limits (usually $0.01\ \tau^{\pm}_m$) have been exceeded. The boundary for the downstream profile will then be moved outward by one grid point if the tolerance has not been met.

The reduced form of the coefficient matrix M is of the band type with nine non-zero diagonals. The linear system can therefore be solved efficiently by one of the many standard routines available through various scientific subroutine packages. The values of U, τ^+ and τ^- at the interior grid points are then contained in the solution vector $\underset{\sim}{s}$.

Our linearization of the numerical scheme also has the effect of uncoupling the continuity equation, and therefore V, from the remaining system. Using equation (2) to eliminate $(\partial U/\partial x)$ from the momentum equation, we obtain

$$- U^2 \frac{\partial}{\partial y} \left(\frac{V}{U}\right) = U_\infty \frac{dU_\infty}{dx} + \frac{\partial \tau}{\partial y} \quad , \tag{44}$$

where all quantities, except V, are now known. Using the initial condition $V(y_c) = 0$, equation (32) can then be integrated outwards from y_c to determine the vertical velocity profile V.

With the values of U, τ^+, τ^- and V known at x_i, the implicit finite difference scheme can be used to advance U, τ^+ and τ^- to x_{i+1}; V is then calculated by equation (44). This process is repeated until a solution over the entire domain of interest is obtained. Alternately, before an increment in the x-direction is made, the current velocity and shear stress profiles can be used to update the linearized coefficients and to improve the solution by iteration.

The proposed numerical scheme is believed to be quite stable, but caution must be exercised to insure the accuracy of the solution. Although the effects of a Goldstein-type singularity at the trailing edge is expected to vanish quickly,[9] a recent study by Burggraf[10] suggests that an extremely fine mesh must be used to insure accuracy in the very near wake region. Typically an x-step size of the order of $R^{-3/5}$, R being the Reynolds number based on chord length, must be used for a mixing length model. Our numerical experiments indicate a comparable x-step size must also be used (for the first 2 or 3% chord length downstream) in the present calculation. Moreover, it is useful to note that the rates of growth for the lower and upper wake edges can be determined by the maximum characteristic angles $\gamma_{-\infty}$ and $\gamma_{+\infty}$ at y_{-L} and y_M. From equation (13) we derive

$$\tan \gamma_{\pm\infty} = \frac{V_{\pm\infty} \pm 2a_1^{\pm} G^{\pm} |\tau_m^{\pm}|^{1/2}}{U_{\pm\infty}} \quad . \tag{45}$$

Thus, the x-step size must also in general be restricted such that the wake width is allowed to expand by no more than one grid point in either normal direction for each x-increment.

RESULTS AND DISCUSSION

As the first test case for our model, we have chosen the measurements by Chevray and Kovasznay of a symmetric wake behind a thin flat plate.[11] The data available in this case is perhaps the most extensive and best documented from both the experimental and the theoretical points of view. The study by Burggraf[9] adapted the Cebeci-Smith and Glushko models to compute the velocity and shear stress profiles and it thus provides a basis of comparison between the present model and other prediction methods now available. It should be noted, however, that due to the use of the eddy viscosity concept, the Cebeci-Smith and Glushko models used by Burggraf are restricted to symmetric flows. The present approach does not assume symmetry in its formulation and a comparison with the asymmetric cascade wake data of Raj and Lakshminarayana[12] is presented as the second test case.

As repeatedly noted in our previous discussions, one of the most crucial steps in the application of the present scheme--or, in fact, any other calculation method--is the choice of empirical functions which define the turbulence structure. In a recent interactive study of symmetric jets and wakes by Morel,[13] a set of empirical functions (see Figure 5) were suggested for wake calculations starting at a point well downstream of the trailing edge. The present solution algorithm has been used to reproduce Morel's results as a check and good agreement was obtained; but Morel's functions are not valid in the near wake region.

It can be argued that the evolution of two coalescing boundary layers into a near wake is initially confined to a region bounded by the two characteristics emanating from the trailing edge.[13] As a first approximation, the boundary layer length scale L is expected to be valid except near the wake center-line where it has been assumed to be constant and proportional to the width of the "inner region"

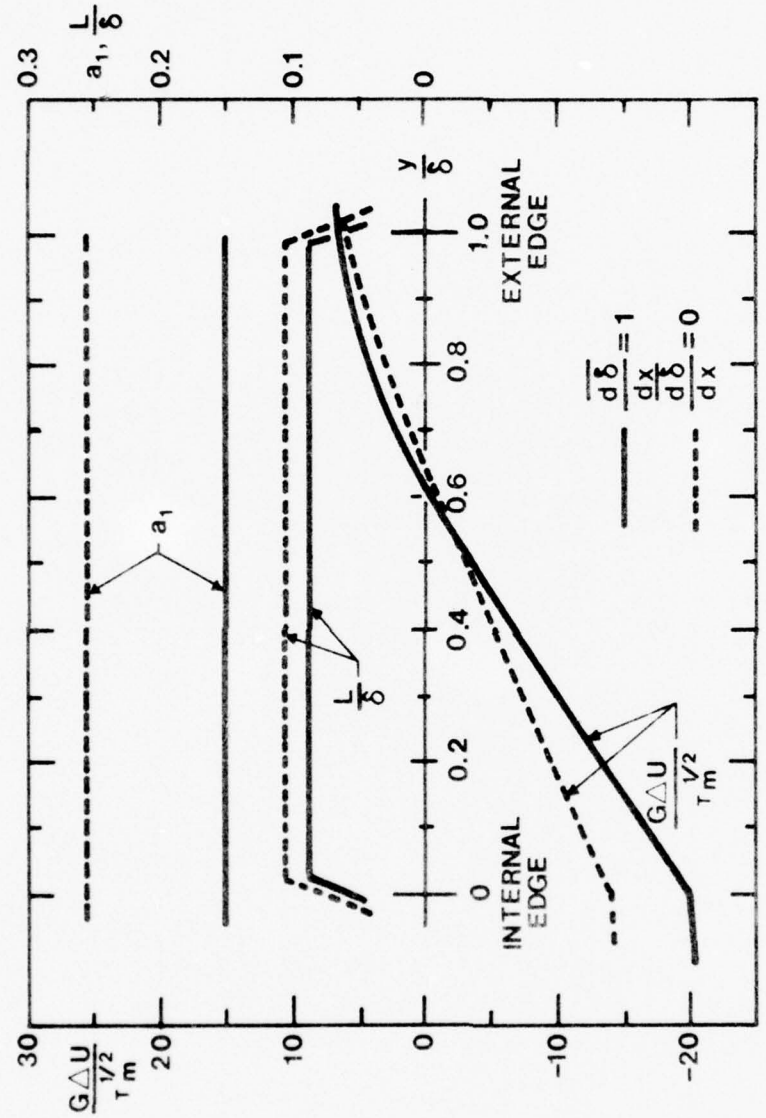

FIGURE 5. EMPIRICAL FUNCTIONS – JETS AND WAKES

(From Morel, 1972)

(see Figure 6). We have tentatively used Morel's function G and the point where G = 0 is correlated with the shear stress maximum. With this normalization, the function G closely approximates its boundary layer counterpart in the outer wake edges but assumes negative values near the wake center-line. This allows the shear stresses to be diffused away from their maxima. The value for a_1 is again taken to be 0.15. The empirical functions used in our present calculations are therefore necessarily crude pending more thorough experimental investigations. In particular, the effects of the assumed "interaction" between the two shear layers must be clarified and incorporated as adjustments in the empirical functions. Nevertheless, the results obtained for the symmetric case are encouraging and they are presented in Figures 7 - 12 along with results obtained by Burggraf based on the Cebeci-Smith and Glushko models. The present method produces good agreements with the experimental velocity profiles at x/θ_0 = 8.6, 34.4 and 86.2 --corresponding to x/c = 0.0208, 0.083 and 0.208 respectively. The predicted shear stress maxima also show improvements over those of Cebeci-Smith and Glushko.

The present model has also been used to compute the asymmetric wake profiles behind a cascade of airfoils at an angle of incidence i = -6°, and comparisons with the experimental measurements of Raj and Lakshminarayana at x/c = 0.08, 0.24 and 0.40 are given in Figures 13 - 18. The empirical functions are exactly those used in the symmetrical case. The inherent asymmetry is accounted for through the previously discussed scaling procedure. The overall agreements between the predicted velocity profiles and the data is good and the present results show considerable improvements over those obtained by either the global or the local similarity methods[14,15]--particularly at the near wake stations. It should be pointed out, however, that the results for the asymmetric case, though satisfactory, do not agree as closely with the experimental results as those for the symmetric case. This is at least in part due to the fact that the observed

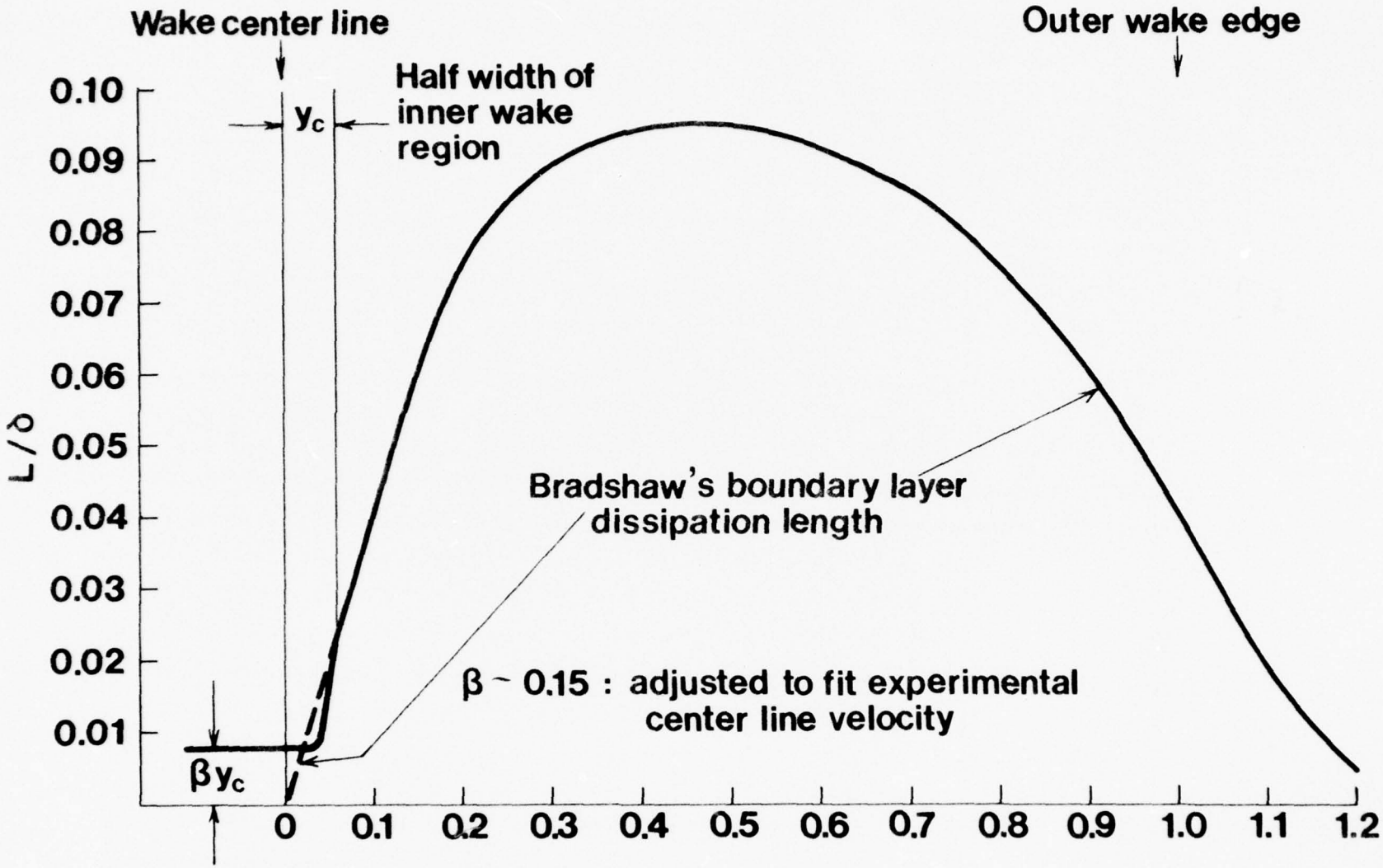

Figure 6. The empirical function L.

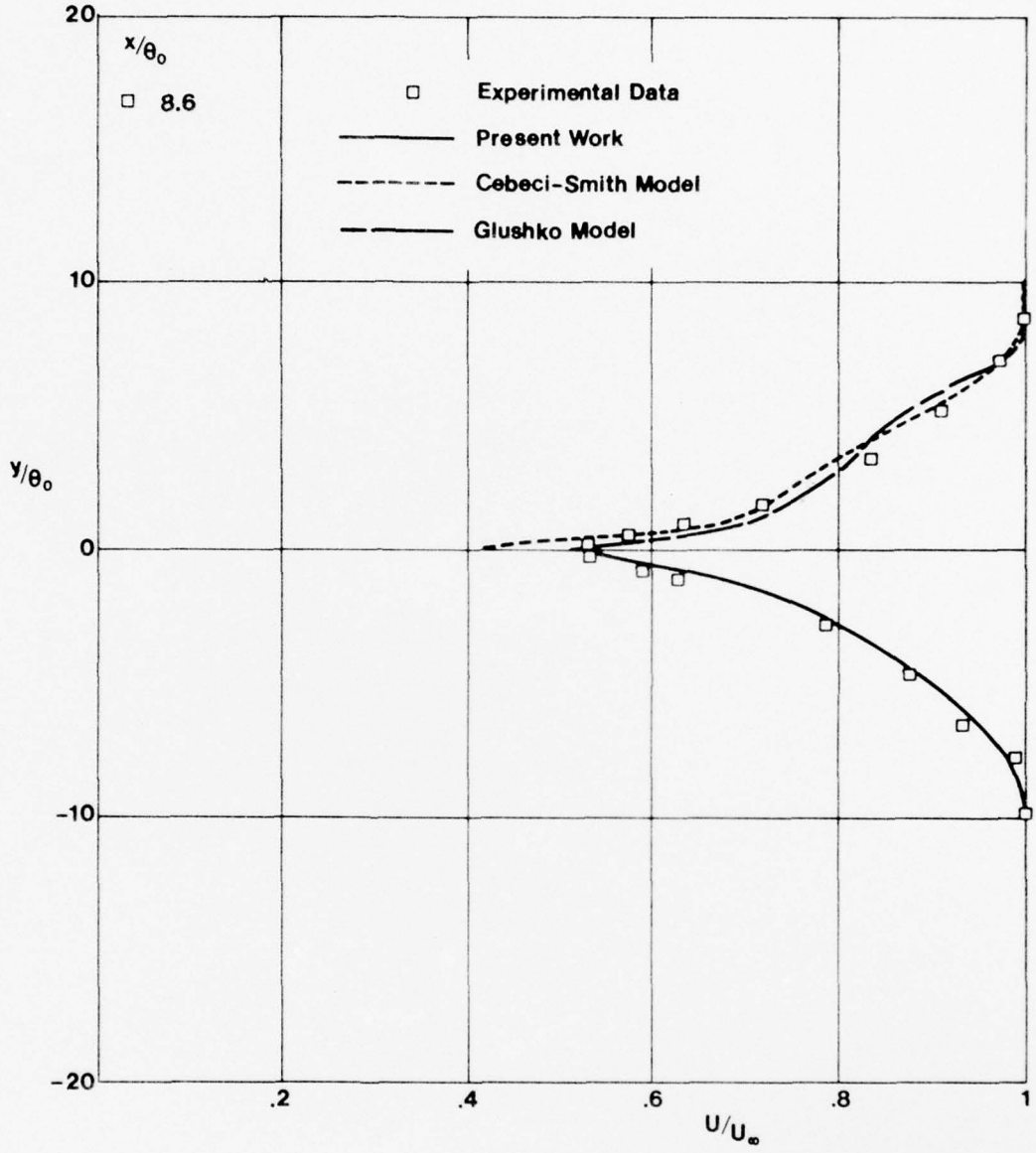

Figure 7
Mean velocity distribution in wake.

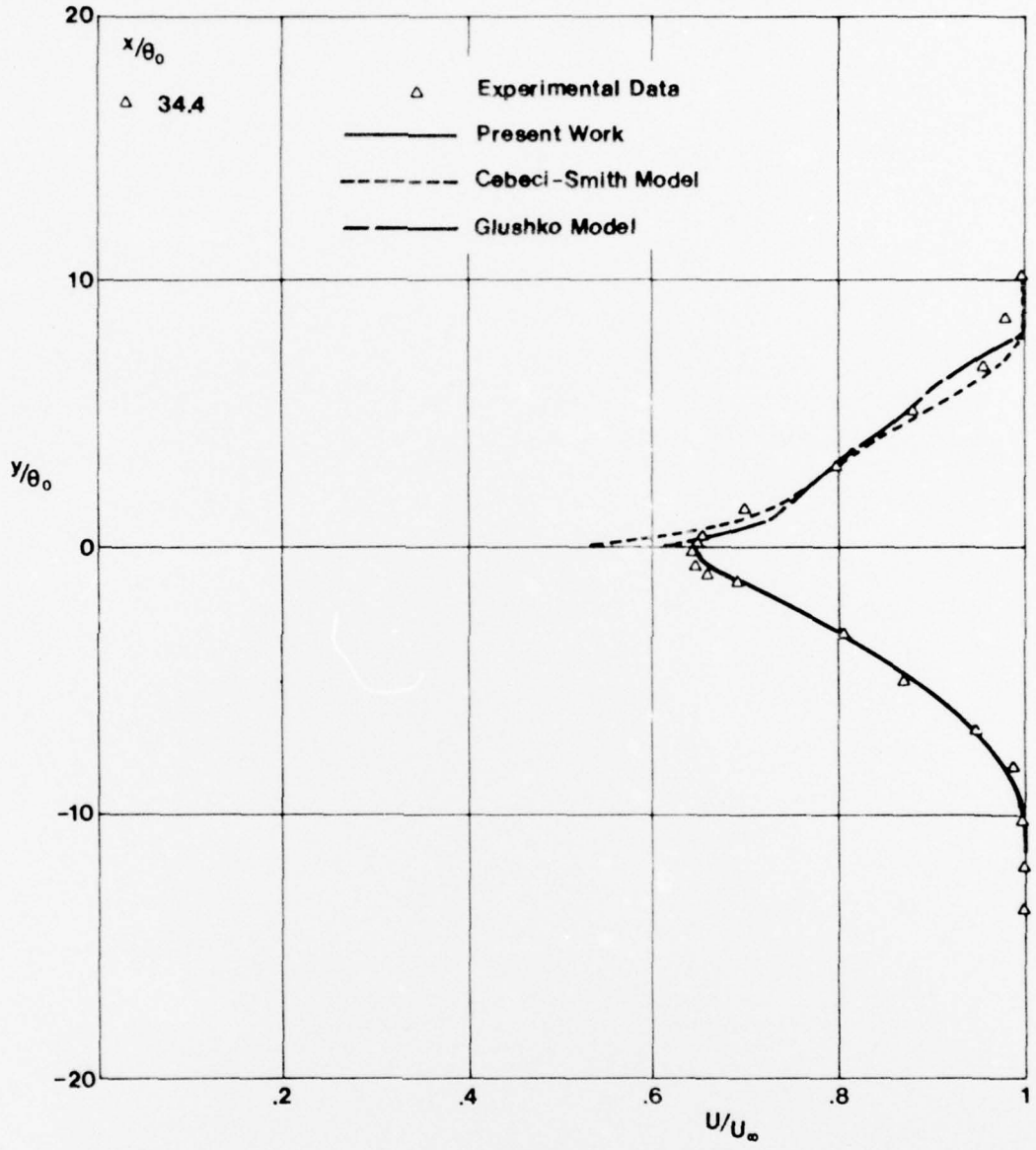

Figure 8

Mean velocity distribution in wake.

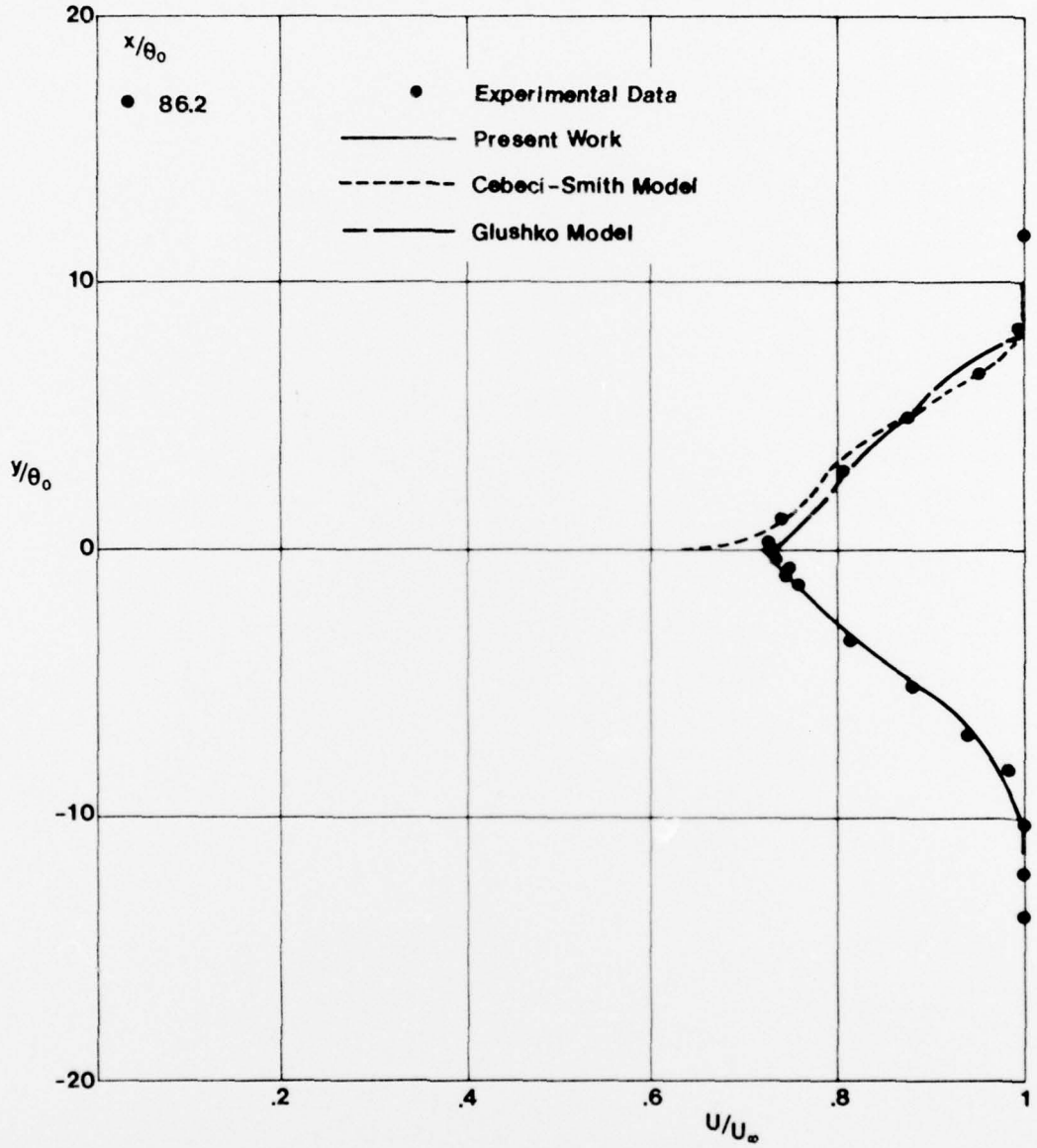

Figure 9

Mean velocity distribution in wake.

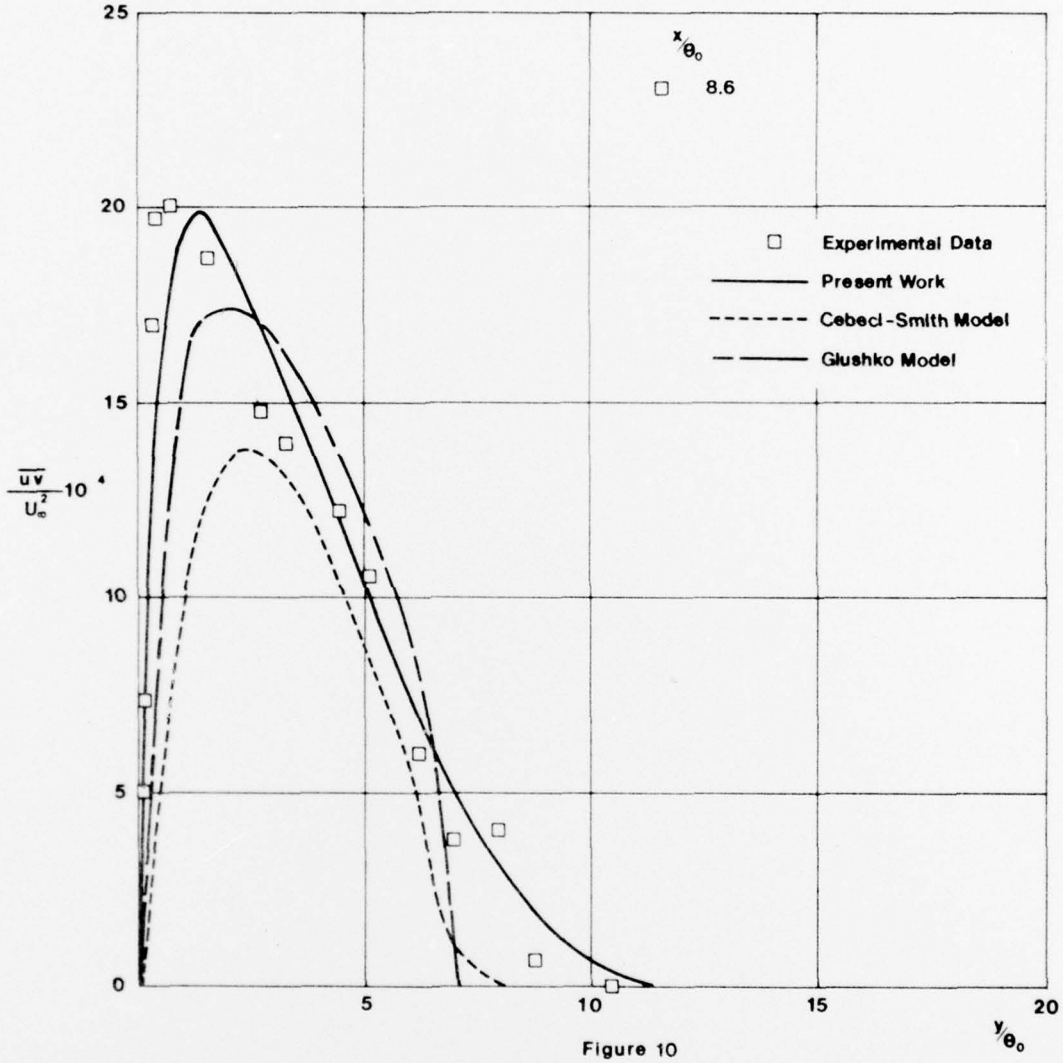

Figure 10
Distribution of Reynolds stress.

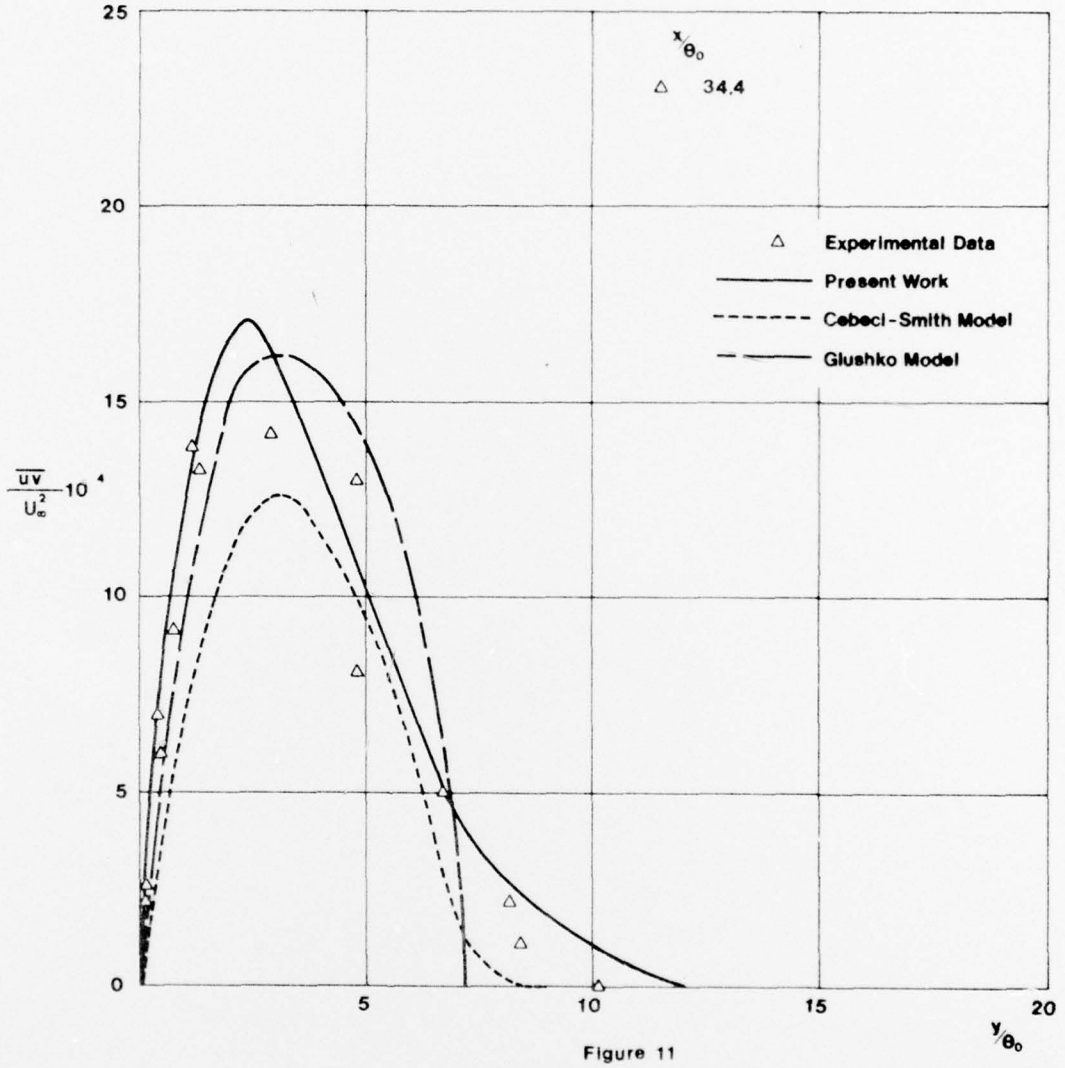

Figure 11
Distribution of Reynolds stress.

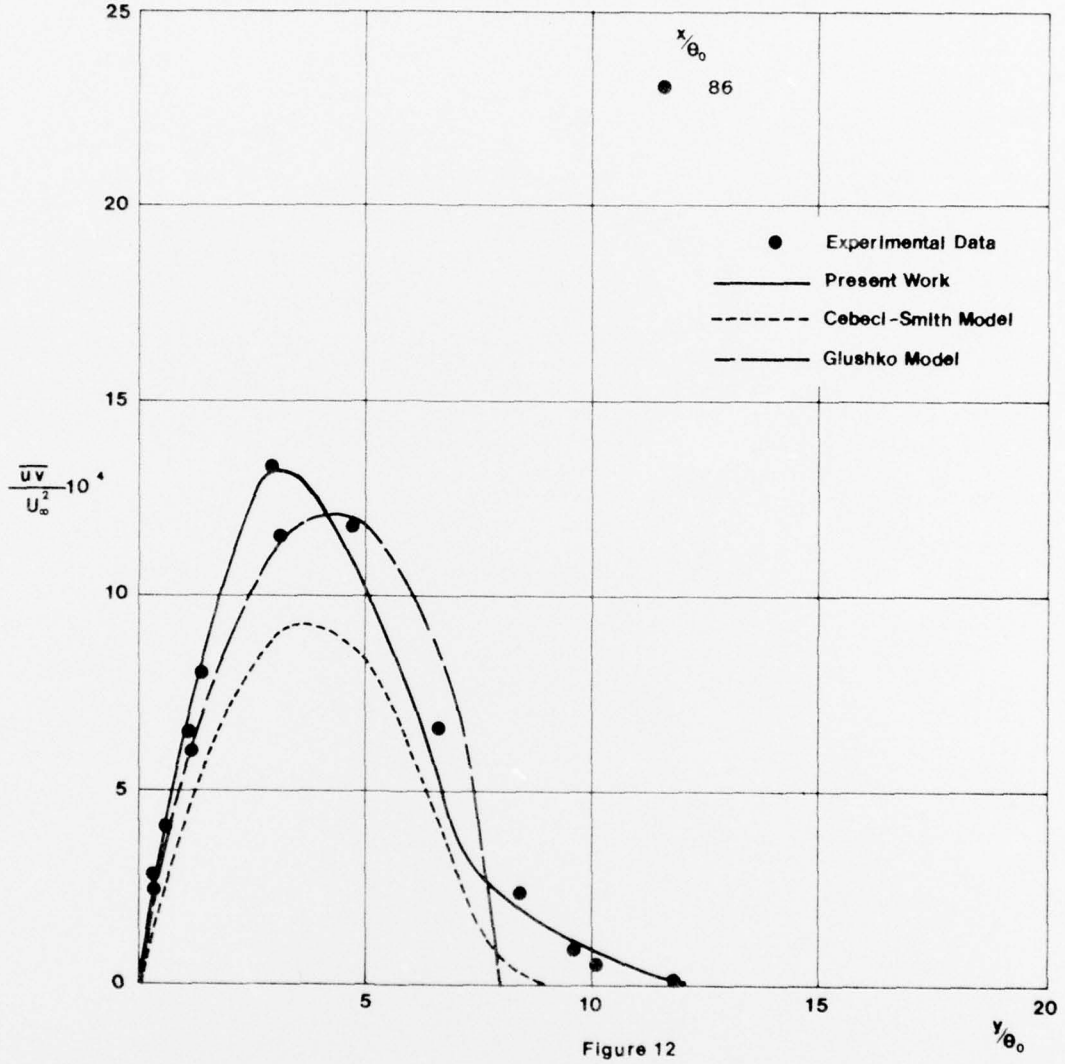

Figure 12

Distribution of Reynolds stress.

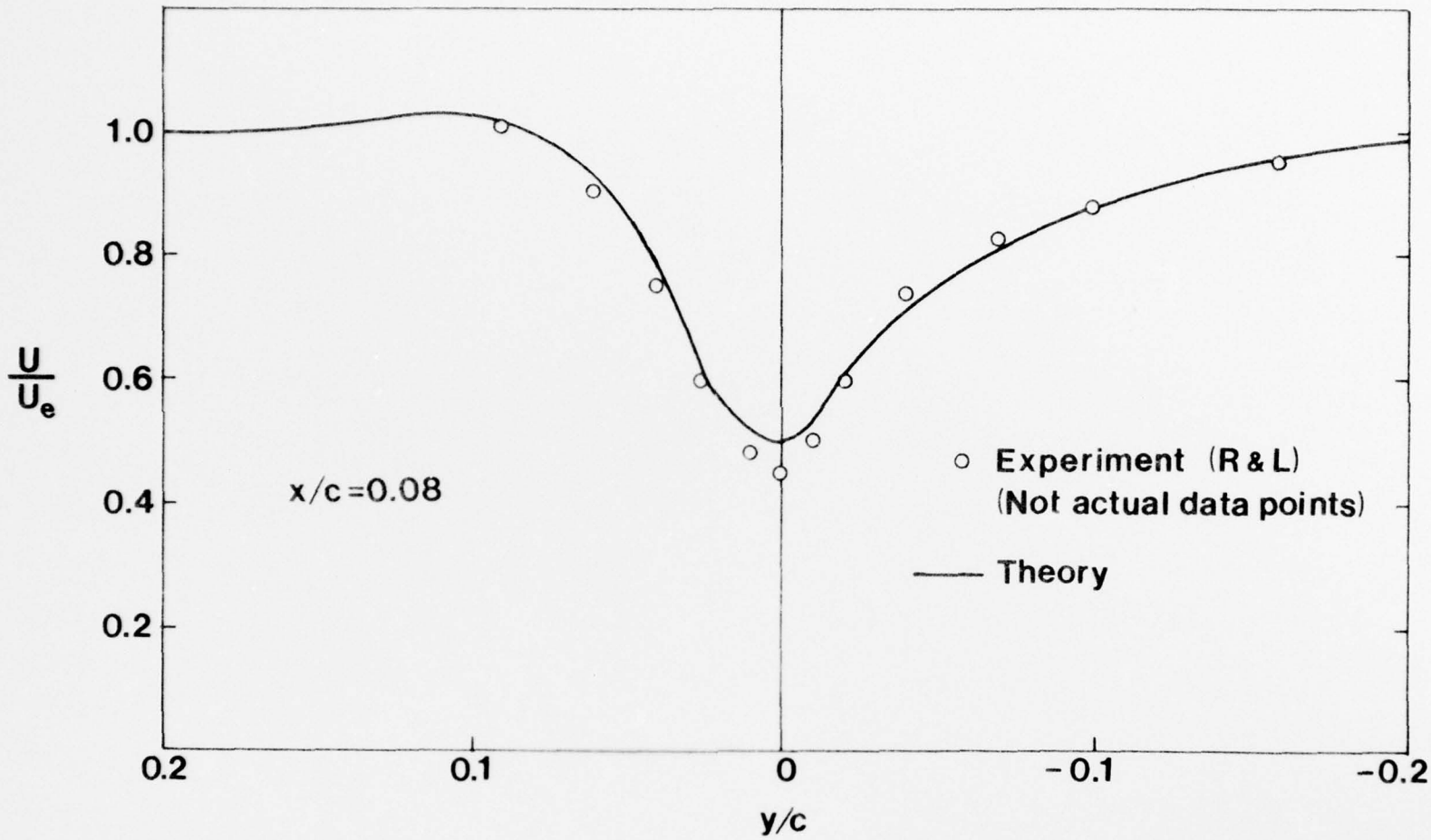

Figure 13. Mean velocity distribution

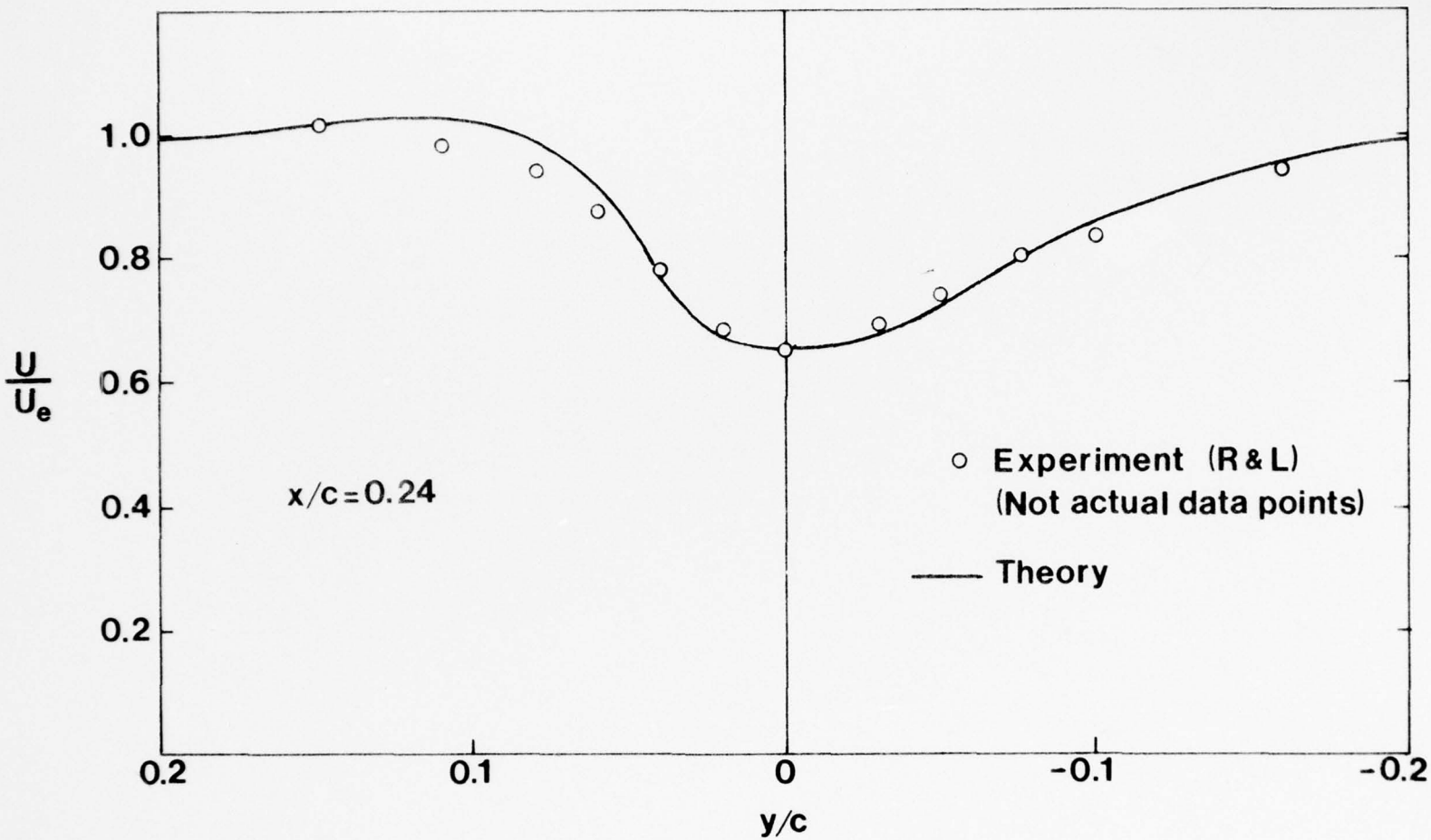

Figure 14. Mean velocity distribution

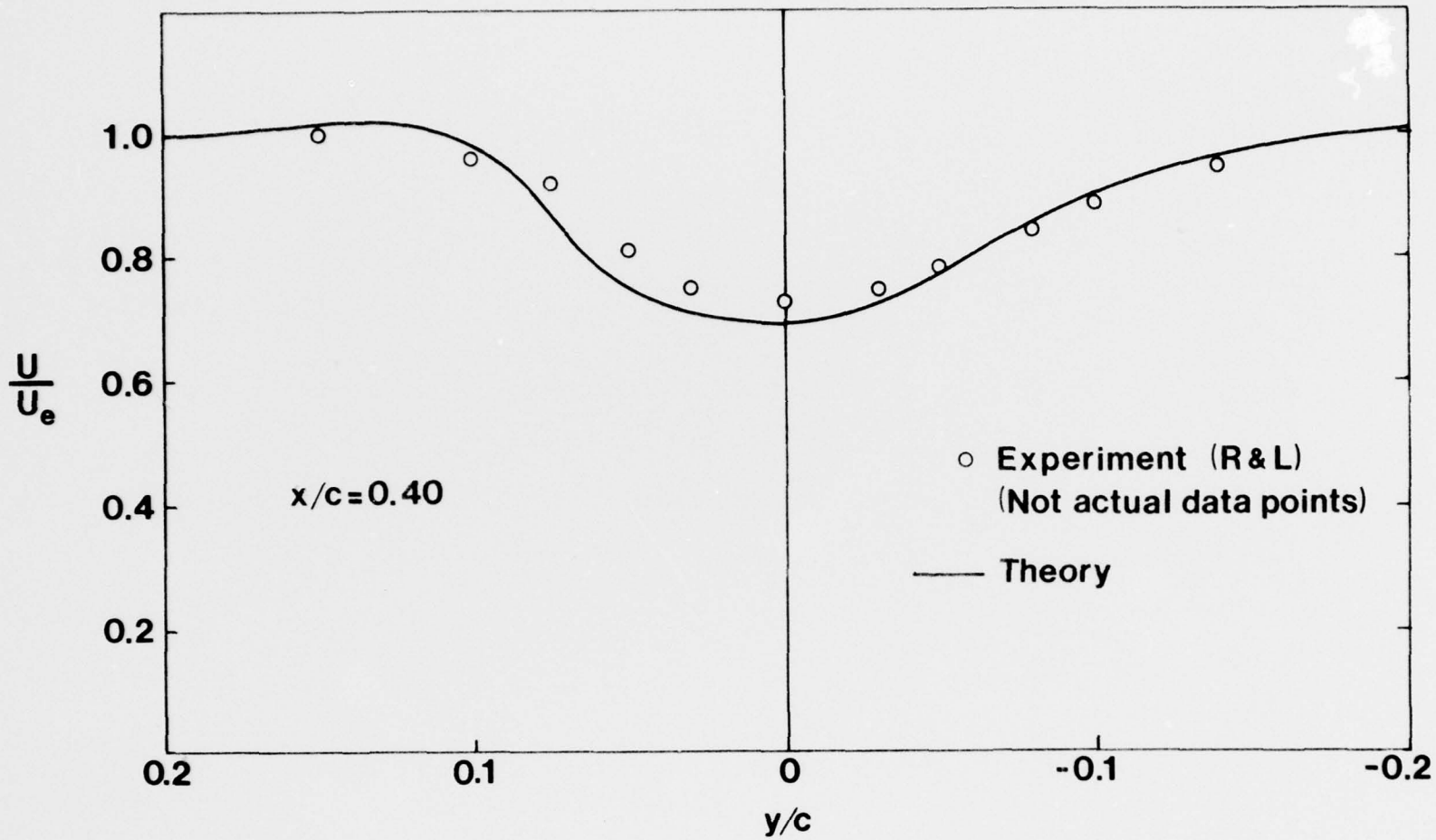

Figure 15. Mean velocity distribution

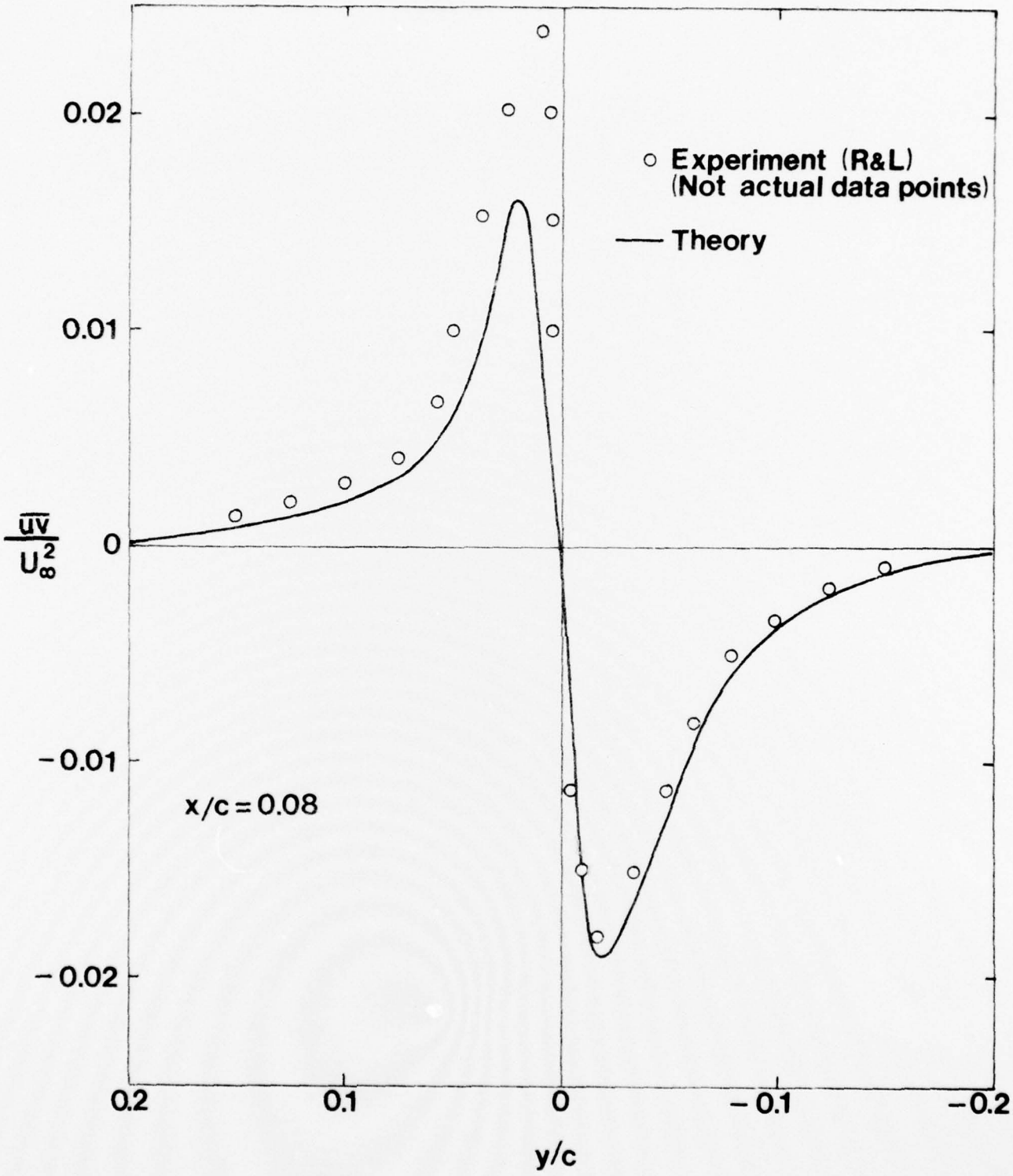

Figure 16. Distribution of Reynolds Stress

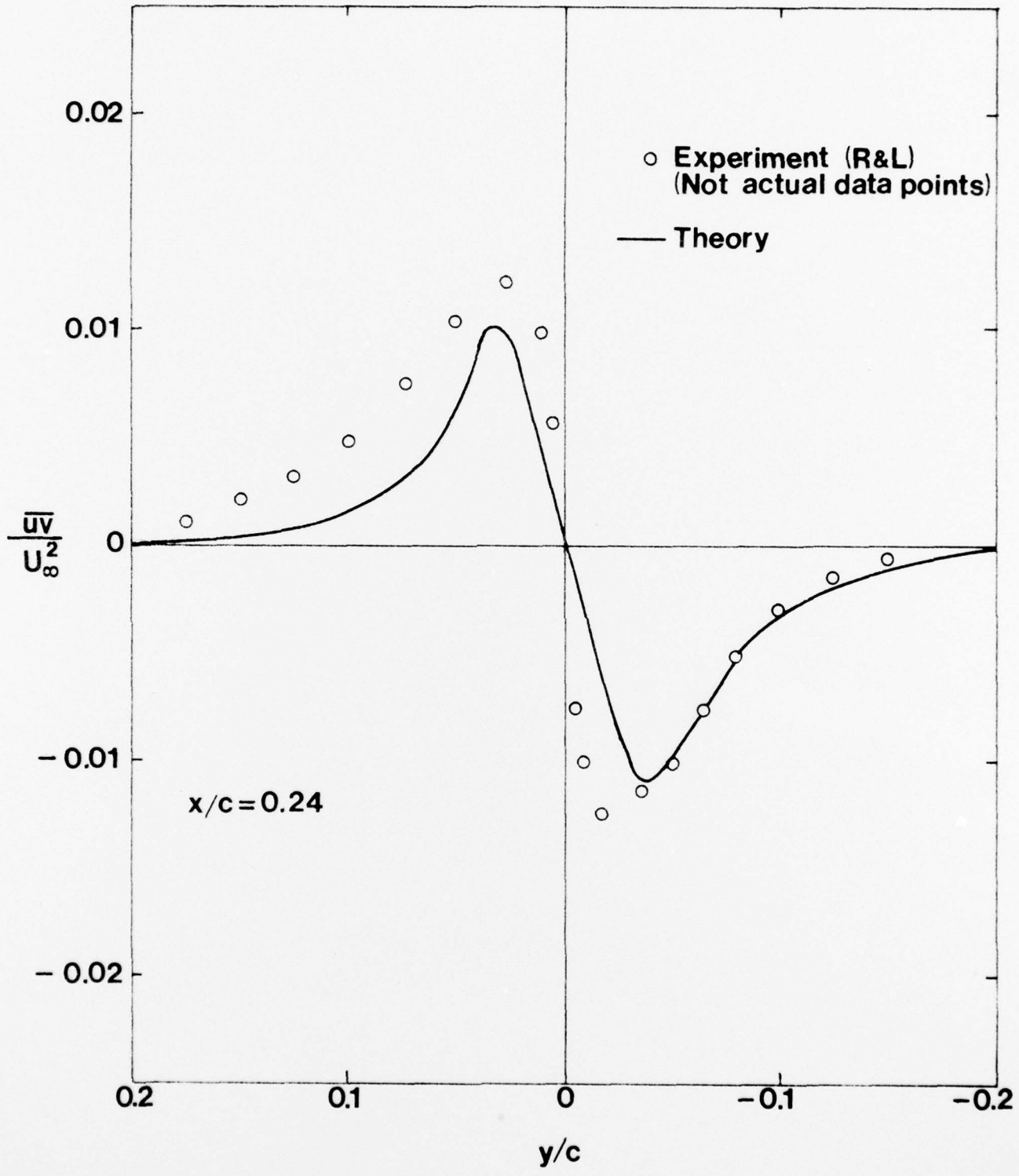

Figure 17. Distribution of Reynolds Stress

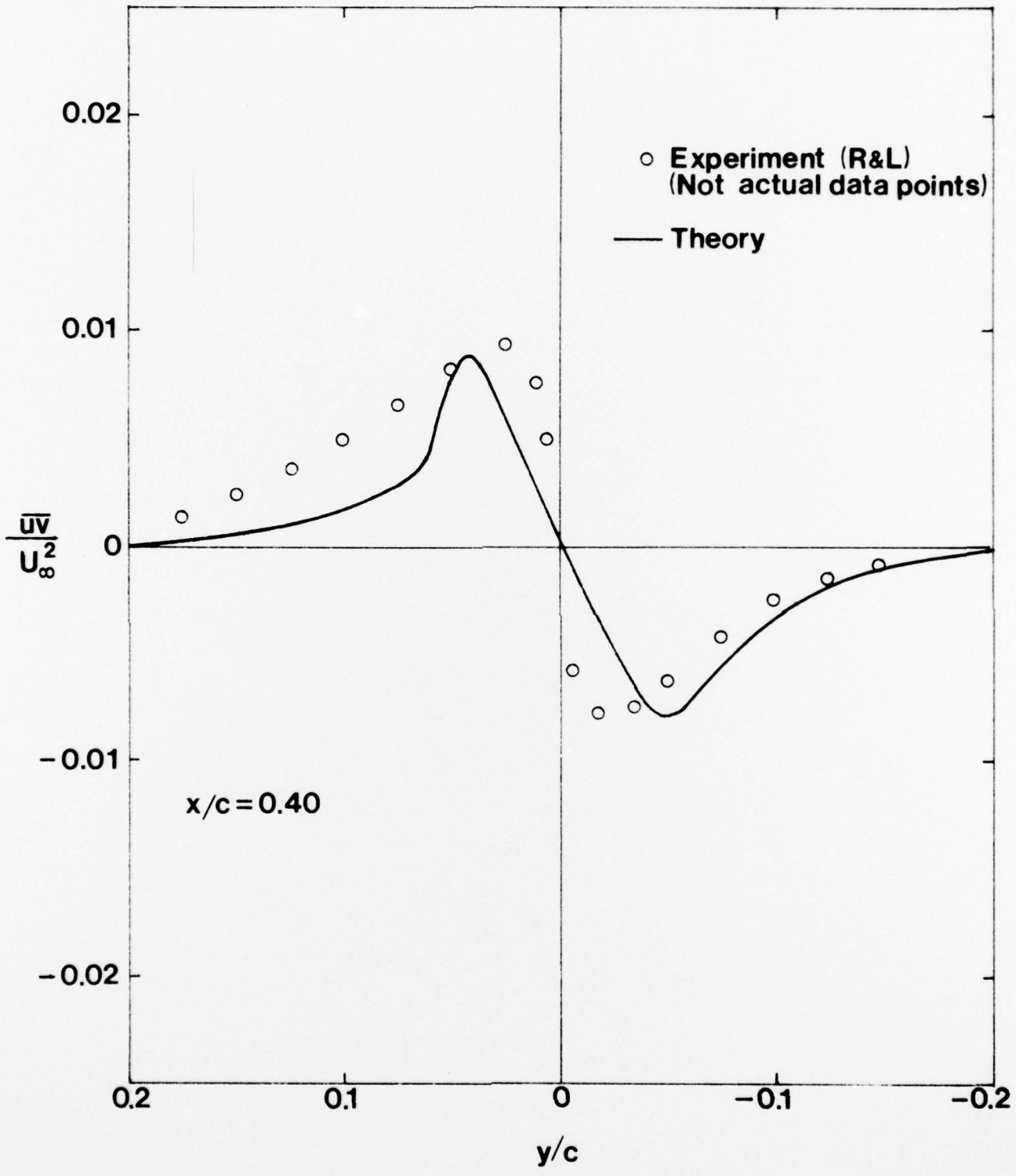

Figure 18. Distribution of Reynolds Stress

turbulent shear stress level for the asymmetric cascade wake is much higher than that for the symmetric case and the accuracy of the empirical functions is more critical. It is also of interest to note that the accuracy of the present model seems to deteriorate as one progresses downstream of the airfoil trailing edge (cf. Figures 16 through 18). The simple adjustments made in the length scale function L in our attempt to account for the evolution of two coalescing boundary layers into a fully developed far wake are perhaps too crude to adequately model this extremely complex and intricate process.

In this connection, it is highly desirable that some detailed experimental measurements with sufficient spatial resolution be carried out in the near future in order to obtain a good data base from which the boundary layer/wake mixing can be quantified and the physical basis for the interaction hypothesis be ascertained. These experiments should also result in a concomittant generation of accurate empirical functions which are correlated to the basic properties of the shear flows.

In summary, our investigation so far has validated the basic philosophy of the interactive approach for near wake calculations, but it also clearly suggests that further refinements in the empirical functions based on reliable experimental data are needed before the present method can be used with confidence as a design tool for an arbitrary, complex, turbulent shear layer.

REFERENCES

1. Kline, S. J., et. al., (ed.) Proceedings, Computation of Turbulent Boundary Layers - 1968 AFOSR - IFP - Stanford Conference, Vol. 1, Stanford University, Thermosciences Division, 1969.

2. Bradshaw, P., et. al. "Calculation of Interacting Turbulent Shear Layers Duct Flow", Journal of Fluids Engineering, Trans. ASME, Series I, Vol. 95, No. 2, 1972, pp. 214-220.

3. Bradshaw, P., et. al. "Calculation of Boundary Layer Development Using the Turbulent Energy Equation", Journal of Fluid Mechanics, Vol. 28, Part 3, 1967, pp. 593-616.

4. Bradshaw, P. and Ferriss, D. H. "Applications of a General Method of Calculatin Turbulent Shear Layers", Journal of Basic Engineering, Trans. ASME, Series D, Vol. 94, No. 2, 1972, pp. 345-352.

5. Bradshaw, P. "Calculation of Boundary-Layer Development Using the Turbulent Energy Equation IX Symmary", NPL Report 1287, Jan., 1969.

6. Bradshaw, P. and Ferriss, D. H. "Calculation of Boundary Layer Development Using the Turbulent Energy Equation: Compressible Flow on Adiabatic Walls", Journal of Fluid Mechanics, Vol. 46, 1967, pp. 83-110.

7. Ferriss, D. H. "An Implicit Numerical Method for the Calculation of Boundary Layer Development Using the Turbulent Energy Equation", NPL Aero Report 1295, 1969.

8. Cebeci, T. and Smith, A.M.O. Analysis of Turbulent Boundary Layers, Academic Press, New York, 1974.

9. Bradshaw, P. "Prediction of the Turbulent Near Wake of a Symmetrical Airfoil", AIAA Journal, Vol. 8, 1970, pp. 1507-1508.

10. Burggraf, O. R. "Comparative Study of Turbulence Models for Boundary Layers and Wakes", Aerospace Research Laboratories, TR-74-0031, March, 1974.

11. Chevray, R. and Kovasznay, L.S.G. "Turbulent Measurements in the Wake of a Thin Flat Plate", AIAA Journal, Vol. 7, No. 8, 1969, pp. 1641-1643.

12. Raj, R. and Lakshminarayana, B. "Characteristics of the Wake Behind a Cascade of Airfoils", J. Fluid Mechanics, Vol. 61, 1973, pp. 707-730.

13. Morel, T. "Calculation of the Free Turbulent Mixing: Interaction Approach", Ph.D. Thesis, Ill. Inst. of Tech., Chicago, 1972.

14. Huffman, G. D., et. al. "A Proposal for Research on Aerodynamically Induced Vibrations in Turbomachines", Indianapolis Center for Advanced Research, 1975.

15. Gustafson, W. A., et. al. "Cascade Wake Structure", Indianapolis Center for Advanced Research, 1975.

PUBLICATIONS RESULTING FROM CONTRACT

1. Fleeter, S., Novick, A. S., and Riffel, R. E., "The Unsteady Aerodynamic Response of an Airfoil Cascade to a Time-Variant Supersonic Inlet Flow Field", AFOSR Technical Report, Detroit Diesel Allison EDR 8524, June 1975.

2. Fleeter, S., Novick, A. S. and Riffel, R. E., "The Unsteady Aerodynamic Response of an Airfoil Cascade to a Time-Variant Supersonic Inlet Flow Field", AGARD-CPP-177, AGARD Conference on Unsteady Phenomena in Turbomachinery, Monterey, California, September 1975.

3. Ng, B. S., and Huffman, G. D., "An Analytical Model of an Asymmetric Turbulent Near Wake Behind an Airfoil", Invited major presentation for Project Squid Workshop on Turbulence in Internal Flows, Washington, D. C. June 1976.

4. Gustafson, W. A., Deffenbaugh, F. D. and Davis, D. W., Jr., "Analysis of the Turbulent Wake of a Cascading Airfoil", submitted for publication in Journal of Aircraft.

5. Ng, B. S. and Huffman, G. D., "Aerodynamically Induced Vibrations in Turbomachines - A Semi-Annual Report", ICFAR-FDL-75-002, September 30, 1975.

6. Fleeter, S., Jay, R. L., and Bennett, W. A., "Compressor Stator Time-Variant Aerodynamic Response to Upstream Rotor Wakes", Detroit Diesel Allison EDR 9005, November 1976.

7. Huffman, G. D., "The Modelling of a Turbulent Near Wake Using the Interactive Hypothesis, AFOSR Final Report, 1976, to be submitted to the Journal of Fluid Mechanics.